NPS-ME-94-001

NAVAL POSTGRADUATE SCHOOL
Monterey, California

MAST-ANTENNA SURVIVABILITY: STRUCTURAL DYNAMIC DESIGN ANALYSIS BY COMPONENT MODE SYNTHESIS

by

Prof. Joshua H. Gordis, Principal Investigator,
Prof. Young S. Shin, Principal Investigator,
LT Lynn J. Peterson, USN

Department of Mechanical Engineering

January 1994

Prepared for:

Naval Sea Systems Command
2531 Jefferson Davis Hwy
Arlington, VA 22242-5160

Naval Postgraduate School
Monterey, California

Real Admiral T. A. Mercer,
Superintendent

H. Shull,
Provost

This report was prepared for and funded by the Naval Sea Systems Command, Arlington, VA 22242-5160.

This report was prepared by:

REPORT DOCUMENTATION PAGE

Form Approved
OMB No. 0704-0188

1. AGENCY USE ONLY *(Leave Blank)*	2. REPORT DATE	3. REPORT TYPE AND DATES COVERED
	January 31, 1994	1 May 1993 - 31 Dec. 1994

4. TITLE AND SUBTITLE

Mast-Antenna Survivability: Structural Dynamic Design Analysis by Component Mode Synthesis

5. FUNDING NUMBERS

6. AUTHOR(S)

Joshua H. Gordis, Assistant Professor,
Young S. Shin, Professor, and
Lynn J. Petersen, LT USN

7. PERFORMING ORGANIZATION NAME(S) AND ADDRESS(ES)

Naval Postgraduate School, Department of Mechanical Engineering
Monterey, CA 93943-5100

8. PERFORMING ORGANIZATION REPORT NUMBER

NPS-ME-94-001

9. SPONSORING/MONITORING AGENCY NAME(S) AND ADDRESS(ES)

Naval Sea Systems Command
2531 Jefferson Davis Highway
Arlington, VA 22242-5160

10. SPONSORING/MONITORING AGENCY REPORT NUMBER

11. SUPPLEMENTARY NOTES

The views expressed are those of the authors and do not reflect the official policy or position of DOD or the U. S. Government.

12a. DISTRIBUTION/AVAILABILITY STATEMENT

Approved for public release; distribution is unlimited.

12b. DISTRIBUTION CODE

13. ABSTRACT *(Maximum 200 words)*

The structural survivability of shipboard mast/antenna systems subjected to underwater explosion can be "designed in," through the determination of the structural dynamics of the mast/antenna system. This report details the specialized application of accurate and efficient analytic methods for the structural dynamic design analysis of shipboard mast/antenna systems. Investigated herein are a class of substructuring methods, generally referred to as component mode synthesis, which provide for the rapid calculation of dynamic response of the mast/antenna structural system to weapons effects. Additionally, the methods also provide for the simulation of live fire testing. The methods allow the individual antennae and the mast to each be independently modeled, arbitrarily combined, and combined system dynamic response rapidly calculated to determine the structural survivability of a proposed mast/antenna configuration. This rapid and "modular" component-based analysis capability is specifically tailored for interactive computer-aided design analysis of shipboard mast/antenne systems.

14. SUBJECT TERMS	15. NUMBER OF PAGES
Structural dynamics, component mode synthesis, mast, antenna, survivability	60
	16. PRICE CODE

17. SECURITY CLASSIFICATION OF REPORT	18. SECURITY CLASSIFICATION OF THIS PAGE	19. SECURITY CLASSIFICATION OF ABSTRACT	20. LIMITATION OF ABSTRACT
Unclassified	Unclassified	Unclassified	

TABLE OF CONTENTS

NOMENCLATURE

A. SYMBOLS

$[\,]$	Matrix
$[\,]^T$	Transpose of a matrix
$[\,]^{-1}$	Inverse of a matrix
$\{\,\}$	Column vector
$\{\,\}^T$	Row vector
$\{F\}$	Vector of point forces/moments on the coupled system in the modal coordinate system
$\{F_I\}$	Vector of interface point forces/moments in the physical coordinate system
$\{F_O\}$	Vector of internal point forces/moments in the physical coordinate system
[G]	Flexibility matrix
[I]	Identity matrix
[K], [M]	Stiffness and mass matrices
$\{p\}$	Vector of physical coordinates
$\{q\}$	Vector of displacements in the modal coordinate system
$\{\ddot{q}\}$	Vector of accelerations in the modal coordinate system
[T]	Transformation matrix used to reduce component mass and stiffness matrices

$\{x\}$	Vector of absolute displacements in the physical coordinate system
$\{\ddot{x}\}$	Vector of accelerations in the physical coordinate system
$[\Lambda]$	Diagonal matrix of natural circular frequencies squared $(rad/sec)^2$
λ	Scalar representing a natural circular frequency (i.e. an eigenvalue) expressed in $(rad/sec)^2$
$[\Phi^C]$	Matrix of static constraint mode shapes
$[\Phi^N]$	Matrix of free interface normal modes
$[\Phi_F^N]$	Matrix of fixed interface normal modes
$[\Psi]$	Matrix of residual flexibility modes
$[\Psi^R]$	Matrix of rigid body modes
ω	Forcing frequency (rad/sec)

B. SUBSCRIPTS / SUPERSCRIPTS & OVERSTRIKES

1	substructure 1
2	substructure 2
B	base coordinates
C	static constraint modes
D	deleted
F	fixed interface
I	interface coordinates
K	kept
N	normal modes
O	internal coordinates
R	rigid body modes

r	reduced
rf	residual flexibility
s	system
u	uncoupled
$\dot{x}$	first derivative
$\ddot{x}$	second derivative

C. ACRONYMS / ABBREVIATIONS

C.C.	Computational Cost
CMS	Component Mode Synthesis
DOF	Degree of Freedom
FE	Finite Element
FEM	Finite Element Methods
FLOPS	Floating Point Operations
LFT&E	Live Fire Test and Evaluation
UNDEX	Underwater Detonation and Explosion

MAST-ANTENNA SURVIVABILITY: STRUCTURAL DYNAMIC DESIGN ANALYSIS BY COMPONENT MODE SYNTHESIS

By

Prof. Joshua H. Gordis, Principal Investigator
Prof Young S. Shin, Principal Investigator
LT Lynn J. Petersen, USN

ABSTRACT

The structural survivability of shipboard mast/antenna systems subjected to underwater explosion can be "designed in," through the determination of the structural dynamics of the mast/antenna system. This report details the specialized application of accurate and efficient analytic methods for the structural dynamic design analysis of shipboard mast/antenna systems. Investigated herein are a class of substructuring methods, generally referred to as component mode synthesis methods, which provide for the rapid calculation of dynamic response of the mast/antenna structural system to weapons effects. Additionally, the methods also provide for the simulation of live fire testing. The methods allow the individual antennae and the mast each to be independently modeled, arbitrarily combined, and the combined system dynamic response calculated to determine the structural survivability of a proposed mast/antenna configuration. This rapid and "modular" component-based analysis capability is specifically tailored for interactive computer-aided design analysis of shipboard mast/antenna systems.

I. INTRODUCTION

This report documents the development of analytic methods for maximizing the combat survivability of shipboard structural systems subjected to weapons effects. Survivability will be improved through the characterization of the mast/antenna system structural dynamics and the development of specialized design analysis tools for the prediction and minimization of dynamic response due to weapons effects. The objective is improved system combat survivability.

Additionally, the methods will be developed in the context of the analytic simulation of live fire test and evaluation (LFT&E) for shipboard systems. Those shipboard structural systems which undergo linear elastic dynamic response due to live fire effects can be evaluated for live fire survivability using the simulation methods to be developed, thereby eliminating the need for actual LFT&E for these systems. Alternatively, these simulations will be of benefit in the planning of actual live fire test and evaluation (LFT&E) programs.

The results herein focus on shipboard mast/antenna structures. Shipboard mast/antenna systems must be designed to withstand moderate to severe shock loading induced by underwater explosion (UNDEX) of conventional or nuclear type. The UNDEX delivers devastating forces to the targets in the form of incident shock wave pressure, gas bubble oscillation, cavitation closure pulses, and various reflection wave effects. These shock-induced forces then propagate through the ship to the various systems, equipment, and top-side structures including the mast and antennae. The response of the mast and antennae to the UNDEX shock wave is basically linear elastic and vibrational in nature. The mast and antennae tend to vibrate at their fundamental natural frequency, or at a low range of natural frequencies. The maximum amplitude of the vibration usually occurs after the shock wave passes the ship. The shock response wave form is remarkably different at various levels within the ship. In essence, the ship

acts as a low pass structural filter which alters the characteristics of the propagating shock wave from one possessing high frequency components to one that contains relatively low frequency components [1] Thus, the shock survivability of the mast/antenna system, which is located top-side, is a vibration problem in which relatively low frequency equipment support excitations are observed. The emphasis on design analysis relates directly to the survival of the mission critical systems on the platform. The ability of the naval vessel to carry out its mission after being subjected to an UNDEX threat depends on the survivability of these systems, and specifically the mast/antenna system.

Combat survivability of new systems, such as the mast/antenna system can be "designed in" by accounting for the structural dynamics of the system during the design process. The methods developed herein focus on the structural dynamics of the mast/antenna systems, so that their combat survivability can be directly addressed in the design process. Additionally, the methods will make possible the improvement of survivability of existing systems. For example, survivability can be improved by dynamically tuning and relocating antennae based on the application of the methods to be described.

A. BACKGROUND

The dynamic response of a shipboard antenna is dependent on the dynamic interaction of the antenna with the mast during response to weapons effect. Large dynamic loads in an antenna can result if (a) the antenna is mounted on the mast at a location with large accelerations due to weapons effects, or (b) the antenna has its natural frequencies in close proximity to the excited natural frequencies of the mast. In recent years, the Navy has had frequent occurrences of shipboard antenna systems failing structurally after being subjected to shock due to weapons effects [2]. In order to design these structural systems (i.e. mast and antenna) for minimum dynamic response and hence maximum survivability, the structural dynamic parameters which determine the dynamic response of the system

must be accurately quantified. The primary structural dynamic parameters to be determined are the *modal parameters* (i.e., natural frequencies, mode shapes, modal mass and damping) of the mast and various individual antennae. The modal parameters are required to characterize the structural dynamics of each substructure, e.g. the mast and each antenna, and hence characterize the dynamics of the combined structural system. Given an accurate coupled system analytic dynamics model, weapons-induced dynamic response can then be predicted, and system designs can be evaluated and optimized with respect to survivability. The coupled system analytic dynamics model can serve as the basis for the computer simulation of LFT&E.

B. OVERVIEW OF THE SUBSTRUCTURE APPROACH TO THE DESIGN ANALYSIS OF MAST/ANTENNA SYSTEMS

The methods described herein are directed at the automated design analysis of mast/antenna systems. The methods provide accurate estimates of the modal parameters for a mast/antenna structural system, and therefore will provide accurate estimates of the dynamic response due to weapons effects. Generally referred to as "component mode synthesis," these substructuring methods make use of independent finite element models for the mast and each antenna. In order to allow a designer to rapidly assess for survivability a large number of candidate mast/antenna system designs, the methods are computationally efficient as well as accurate. With respect to mast/antenna systems, the component mode synthesis process will allow a designer to analytically "install" the various antenna models into the mast model, and rapidly calculate coupled mast/antenna system UNDEX dynamic response. When incorporated into a computer-aided design environment, the complexities of the calculation will be transparent to the designer, and will allow the incorporation of self-checks and protection against user error and misuse.

The substructure approach to mast/antenna structural dynamic analysis can be briefly outlined as follows:

- A designer either finds the dynamic characteristics of the various antennae to be installed from a "catalog" (database) of antenna modal parameters, or calculates individual antenna modal parameters from a finite element model of the antenna. The modal parameters of the antenna constitute the antenna dynamic model.
- The various antennae dynamic models are analytically coupled with the mast model, and the dynamic response of the coupled mast/antenna system due to weapons effects is calculated. If unacceptable dynamic response levels are calculated, the various antennae models can be rapidly repositioned on the mast, or exchanged with other antennae, and the new dynamic response calculated.

This scheme has several significant advantages for the automated design analysis of mast/antenna systems. The primary advantages include:

- The ability of these methods to treat the mast and antennae as "substructures," and arbitrarily and repeatedly combine them for the rapid calculation of dynamic response will make possible the evaluation of a greater number of mast/antenna configurations, and hence will greatly facilitate the determination of an optimal configuration with respect to combat survivability.
- The various masts and antennae are fabricated by various independent contractors. The component mode synthesis method allows the separate modeling of the mast and antennae, and therefore naturally preserves the independence of the contractors.
- The formulations to be described are modal, and therefore can function equally well with analytically derived modal parameters, or with modal parameters identified in a vibration test.

The analytic methods for the generation of the coupled mast/antenna model are the focus of this work. To be evaluated in this report are several component mode methods for substructure synthesis: the Craig-Bampton method and two residual flexibility formulations. The methods are specialized for the mast/antenna analysis problem, and their relative merits compared in the context of combat survivability. The methods are based on the modal representation of components; that is, rather than representing a structure using the mass and stiffness matrices generated in a finite element model, these methods employ various classes of "mode shapes" to represent the substructures or components. For example, the familiar normal modes of vibration are one class of mode shape used.

The computational efficiency of these methods, which is critical to their effectiveness in a computer aided design environment, comes from their ability to accurately describe a component with a minimum number of mode shapes. The sections of this report which follow will describe the above mentioned synthesis formulations, and demonstrate their relative accuracy and efficiency in the calculation of the dynamic response of a small yet representative mast/antenna model, subjected to a variety of applied harmonic forces as well as deck accelerations and displacements. The model used, which includes a mast and a single antenna, is of a small size compared with that required to represent an actual mast/antenna structure. However, the model has all the features necessary to allow the assessment and critical analysis of the component mode synthesis methods.

Specifically, the three synthesis methods will each be used in the following analyses:

(1) Calculation of mast/antenna coupled system modal parameters: This is the fundamental assessment of a method's accuracy. Prior to performing the synthesis, modal parameters are calculated for the antenna model and the mast model. The appropriate component representation is generated and the mast/antenna system is synthesized. The coupled system natural frequencies are calculated and are compared with the natural frequencies calculated using a standard finite element procedure. The standard finite

element procedure means the assembly of a single model representing the total mast/antenna system. A comparison of floating point operations (FLOPS) accumulated in all cases is also provided. This comparison will demonstrate the computational advantage of the synthesis methods, an advantage critical to the development of an automated design analysis system.

Using the synthesized mast/antenna model, the following analyses are presented.

(2) Calculation of antenna peak displacement due to harmonic forcing: A simple harmonic forcing function is applied to the mast and the peak displacement of the antenna free end ("tip") is calculated, again using all three component mode synthesis methods, as well as using a standard finite element procedure.

(3) Calculation of mast/antenna interface internal stresses due to harmonic forcing: A simple harmonic forcing function is applied to the mast and the bending moment and shear loads in the mast/antenna connection are calculated. Note that these internal loads are directly proportional to stress, and hence are the critical quantities which must be calculated in order to assess structural survivability. These calculations are repeated for all three synthesis formulations, as well as for the standard finite element procedure.

II. FORMULATION OF FINITE ELEMENT MODEL AND GENERAL COMPONENT COUPLING PROCEDURES

As discussed in the Introduction, the finite element (FE) procedure will be employed to generate mathematical models of the components (substructures) involved, namely the mast and the antenna. The FE procedure produces stiffness, mass, and less commonly, damping matrices which represent the structural dynamics of each component. In order to faithfully capture the geometric and material complexities of these components, the finite element discretization must necessarily involve many degrees-of-freedom (DOF), and hence the above mentioned system matrices can be quite large. The time and cost associated with the extraction of the modal parameters (natural frequencies, mode shapes, and modal mass) from these large matrices precludes the performance of the repeated design analyses required to arrive at an optimal design. The component mode synthesis methods bypass the repeated extraction of the modal parameters for a complete mast/antennae system by directly using the modal parameters calculated for each component. The calculation for the component "modes" is performed once for each component, and the total system dynamics are synthesized using the various sets of modes so calculated. The synthesis methods not only provide very accurate predictions of dynamic response, but also provide a substantial decrease in the time required to compute dynamic response, hence allowing the performance of additional design analysis iterations.

A. FINITE ELEMENT FORMULATION

Although FE modeling typically involves the full range of element types available (e.g. beam, plate, shell), for purposes of this report the antenna and the mast will each be modeled using beam elements only. This model, although simple, is all that is necessary to

investigate the various component coupling procedures. All methods presented herein are applicable to any structural model, and the results and conclusions presented are directly applicable to the analysis of structural systems of any complexity.

Traditionally, the mast and antennae are modeled together as a system. Alternatively, the mast and antennae can be modeled separately. By modeling the mast and antennae separately, several benefits arise:

- Masts and antennae are generally fabricated by different defense contractors. Therefore, modeling the mast and antennae separately would best preserve this independence.
- Modeling the mast and antennae separately would permit the development of a single data file containing only mast design specifications, and several separate data files containing antenna design specifications, one datafile for each antenna. With this modular, component-based approach comes the flexibility of exchanging antennae and/or changing antenna placement. This allows the rapid assessment of many mast and antenna configurations for dynamic response characteristics.
- By modeling the mast and antennae separately, the computational efficiency increases as compared to modeling the mast and antennae together. This computational advantage is due to the fact that the cost associated with the calculation of the modal parameters for a single structural model is proportional to the cube of the number of DOF of the model [3]. The calculations performed herein demonstrate this comparison between a total mast/antenna model and a model derived from the synthesis of mast and antenna substructure models. The benefit is associated not just with the calculation of the modal parameters, but also with the calculation of dynamic response to assess UNDEX survivability.

B. GENERAL COMPONENT COUPLING PROCEDURES

The term "component mode synthesis" refers to the manner in which each substructure is mathematically represented prior to coupling, and is based on a truncated modal expansion. This representation is most familiar in the context of the calculation of dynamic response. Here, the dynamic response of a structure can be written as a linear combination of the mode shapes calculated for the structure. If the frequency range of excitation is contained in the frequency range of the calculated modes, then the dynamic response calculated using the modes will be of acceptable accuracy. Of course, the question of how many modes to retain is non-trivial and problem specific. However, the computational efficiency of a modal approach to structural dynamics including the component mode synthesis methods to be presented, comes from the retention of a number of modes which constitute a mathematical model much smaller than the original mass and stiffness matrices from which the modes were calculated.

Component mode synthesis makes use of several types of vibrational mode shapes, distinguished by the boundary conditions imposed on the substructure prior to the calculation of these mode shapes. In addition to these vibration mode shapes, the various component mode synthesis methods require additional types of mode shapes to be calculated and included with the vibration modes. Therefore, the term "component mode synthesis" (CMS) is a suitable name: a single structure is synthesized from separate substructures and each substructure is mathematically represented by an appropriate set of mode shapes calculated from the finite element model of each substructure. The following are definitions of the various types of mode shapes that are used in the component mode synthesis formulations investigated herein.

1. FREE INTERFACE NORMAL MODES

The free interface normal modes are the modes of the component when unrestrained at all interface degrees of freedom. The interface coordinates are denoted by the subscript "I" and the internal coordinates are denoted by the subscript "O". The interface coordinates "I" are the coordinates where the substructures are coupled The internal coordinates are all coordinates that are not interface coordinates. Free interface normal modes are calculated by solving the following eigenvalue problem:

$$[K - \lambda \cdot M]\{\Phi^N\} = \{0\} \tag{1}$$

The stiffness and mass matrices in Eq. (1) are partitioned as follows:

$$[K] = \begin{bmatrix} K_{OO} & K_{OI} \\ K_{IO} & K_{II} \end{bmatrix} \qquad [M] = \begin{bmatrix} M_{OO} & M_{OI} \\ M_{IO} & M_{II} \end{bmatrix}$$

The number of equations defined by Eq. (1) is equal to the number of rows or columns in the mass and stiffness matrices. The number of columns or rows in [K] or [M] equals the number of DOF of the component in physical coordinates.

2. FIXED INTERFACE NORMAL MODES

The fixed interface modes are the modes of the component restrained at its interface degrees of freedom. The fixed interface normal modes have the following form:

$$[\Phi_F^N] = \begin{bmatrix} \Psi^N \\ 0 \end{bmatrix}$$

The mode shapes in the upper partition of the matrix of fixed interface normal modes, or $\{\Psi^N\}$, are obtained from the solution to the following eigenvalue problem:

$$[K_{OO} - \lambda \cdot M_{OO}]\{\Psi^N\} = \{0\} \tag{2}$$

In words, the matrix of fixed interface normal modes is a partitioned matrix consisting of the mode shapes obtained from the solution of Eq.(2) in the upper partition, and a matrix of zeros in the lower partition. The zeros mean zero displacement at the interface. The number of rows of the matrix of zeros is equal to the number of interface coordinates, while the number of columns is equal to the number of internal coordinates of the substructure.

Both the free interface normal modes and the modes obtained in the solution to Eq.(2) are unity modal mass normalized such that the following property is satisfied:

$$[\Phi^N]^T [M][\Phi^N] = [I] \tag{3}$$

$$[\Psi^N]^T [M_{OO}][\Psi^N] = [I] \tag{4}$$

3. STATIC CONSTRAINT MODES

Static constraint modes are calculated by enforcing a unit deflection on each interface DOF while holding all other DOF restrained. Calculating the resulting displacements of the internal coordinates defines the static constraint modes. If it can be assumed that no external forces or inertial forces are applied to the internal degrees of freedom, as in a static's problem, the shapes, or $[\Phi^C]$, can be calculated from the stiffness matrix as follows:

$$\begin{Bmatrix} x_O \\ x_I \end{Bmatrix} = [\Phi^C]\{x_I\} = \begin{bmatrix} -K_{OO}^{-1} K_{OI} \\ I \end{bmatrix} \{x_I\} \tag{5}$$

4. RIGID BODY MODES

Rigid body modes are associated with systems that are not constrained. Rigid body modes have zero frequency. They can be solved for using equation (2). They can also be solved for in a manner identical as that for static constraint modes, provided that the number of coordinates retained is equal to the number of rigid body modes. For purposes this report, rigid body modes will be solved for in accordance with equation (5).

5. RESIDUAL FLEXIBILITY MODES

Before defining "residual" flexibility, the concept of flexibility must first be defined The flexibility of a restrained structure (i.e. a structure whose stiffness matrix is of full rank) is the inverse of the stiffness of the structure. By inverting the stiffness matrix, one obtains the flexibility matrix as follows:

$$[G] = [K]^{-1} \tag{6}$$

Equation (6) can also be written as follows:

$$[G] = [\Phi^{N}][\Lambda]^{-1}[\Phi^{N}]^{T} \tag{7}$$

The residual flexibility matrix is obtained from the flexibility matrix, the kept free interface normal modes, and the inverse of the natural frequencies as follows:

$$[G^{rf}] = [G] - [\Phi_{k}^{N}][{}^{1}\Lambda_{K}]^{-1}[\Phi_{k}^{N}]^{T} = [\Phi_{D}^{N}][{}^{1}\Lambda_{D}]^{-1}[\Phi_{D}^{N}]^{T} \tag{8}$$

The residual flexibility modes are the portion of the exact static flexibility shapes that are not represented by a set of retained modes. Residual flexibility modes require the

knowledge of other modes that are retained in the model and are dependent upon the retained modes. There are two ways to calculate the residual flexibility modes.

1) If the structure is grounded, such as the mast, then the stiffness matrix is full rank and invertible. By post-multiplying Eq. (8) by $\begin{bmatrix} 0_{OI} \\ I_{II} \end{bmatrix}$ one obtains the residual flexibility modes for restrained substructures.

$$[\Psi] = [G^{rf}] \begin{bmatrix} 0_{OI} \\ I_{II} \end{bmatrix} \tag{9}$$

2) However, If the component is not grounded before assembly, such as an antenna, then an inertia relief solution must be calculated to determine the flexibility matrix as follows:

$$[G] = \left[I - \Psi^R \Psi^{R^T} M\right]^T [K^*] \left[I - \Psi^R \Psi^{R^T} M\right] \tag{10}$$

where Ψ^R are the rigid body modes of the structure.

[K *] is formed by inverting the restrained or internal degrees of freedom in the system in the following way:

$$[K^*] = \begin{bmatrix} 0 & 0 \\ 0 & K_{OO}^{-1} \end{bmatrix} \tag{11}$$

This "new" [G] or flexibility matrix in Eq.(10) is free of rigid body modes. The Craig-Chang formulation, which will be presented in the next section uses free-interface normal modes and residual flexibility modes. The residual flexibility modes of unrestrained substructures are obtained from the neglected or deleted free interface normal modes just like they were obtained from a substructure that is restrained. The only difference is that

the flexibility matrix obtained in Eq. (10) is used. Residual flexibility modes are calculated by computing the static flexibility and subtracting the flexibility due to the retained modes. The residual flexibility modes are obtained from the flexibility matrix in Eq.(10) in the same way that they were obtained in Eq.(9):

$$[\Psi] = [G^{rf}] \begin{bmatrix} 0_{OI} \\ I_{II} \end{bmatrix} \tag{12}$$

III. COMPONENT MODE SYNTHESIS FORMULATIONS

A. CRAIG-BAMPTON FORMULATION

There are three substructure coupling procedures that serve as potential candidates to be used in the mast/antenna synthesis. The Craig-Bampton formulation, the Craig-Chang residual flexibility method, and the MacNeal residual flexibility method. In this section, the Craig-Bampton formulation will be presented, while in Section B the Craig-Chang and MacNeal residual flexibility methods will be presented together because of the similarities in the methods.

The Craig-Bampton reduction procedure uses a combination of static constraint modes and fixed interface normal modes to represent the component model. Both the static constraint modes and the fixed interface normal modes are obtained from the finite element substructure models. This combined set of mode shapes will be used to transform the original large order substructure mass and stiffness matrices down to a significantly smaller size, a size equal to the number of mode shapes included in the transformation matrix. The transformation matrix, $[T_1]$, for the Craig-Bampton formulation contains the shape functions as its columns as follows:

$$\begin{Bmatrix} x_O \\ x_I \end{Bmatrix} = \begin{bmatrix} -K_{OO}^{-1}K_{OI} & \Psi^N \\ I & 0 \end{bmatrix} \begin{Bmatrix} x_I \\ q \end{Bmatrix} = [T_1] \begin{Bmatrix} x_I \\ q \end{Bmatrix} \tag{13}$$

This transformation matrix is obtained for each substructure in the system. The size of the static constraint mode partition of the transformation matrix is always fixed, because the number of columns corresponds to the number of interface degrees of freedom. However, the fixed interface normal mode partition is not held constant. The number of

columns can range as low as one column if only one fixed interface normal mode is retained, or as high "m" columns where "m" is the total number of internal degrees of freedom. The size of the transformation matrix depends upon how many modes are required to accurately represent the physical dynamic response of the system when subjected to a forced input. Retaining fewer modes than the total possible modes available is referred to as "modal truncation," and provides the computational efficiency of the method. Retaining fewer modes than the total amount of modes available means fewer calculations required in conducting the dynamic analysis. On the other hand, if the number of modes retained are not sufficient to accurately determine the dynamic response, then the benefits of reduced compute times do not outweigh the magnitude of error obtained in the analysis. Therefore, while the benefits of modal truncation are important in shortening compute times, they are not as important as obtaining accurate results. In terms of computational efficiency, large benefits can be achieved using this method if only the lower range of frequencies is of interest. This is applicable to the mast which is subjected to typically low forcing frequencies. By retaining a few of each of the component modes, an accurate assessment of the dynamic response of the mast and antenna is obtained. The examples contained in section IV and V demonstrate how by retaining just a few modes of each substructure, accurate results can be obtained.

By pre- and post-multiplying the respective substructure mass and stiffness matrices by the transformation matrix in the following manner, one obtains the reduced component model as follows:

$$[K_r] = [T_1]^T \begin{bmatrix} K_{OO} & K_{OI} \\ K_{IO} & K_{II} \end{bmatrix} [T_1] = \begin{bmatrix} K_r^1 & K_r^2 \\ K_r^{2^T} & K_r^3 \end{bmatrix} \tag{14a}$$

$$[M_r] = [T_1]^T \begin{bmatrix} M_{OO} & M_{OI} \\ M_{IO} & M_{II} \end{bmatrix} [T_1] = \begin{bmatrix} M_r^1 & M_r^2 \\ M_r^{2^T} & M_r^3 \end{bmatrix} \tag{14b}$$

The partitions of the reduced mass and stiffness matrices are expressed as follows:

$$K_r^1 = [\Lambda_{KK}]$$
$$K_r^2 = K_r^{2^T} = [0]$$
$$K_r^3 = [K_{II} - K_{IO} K_{OO}^{-1} K_{OI}]$$

$$M_r^1 = [I_{KK}]$$
$$M_r^2 = M_r^{2^T} = [\Psi_{OK}^T (M_{OO}(-K_{OO}^{-1} K_{OI}) + M_{OI})]$$
$$M_r^3 = [(-K_{OO}^{-1} K_{OI})^T (M_{OO}(-K_{OO}^{-1} K_{OI}) + M_{OI}) + M_{IO}(-K_{OO}^{-1} K_{OI}) + M_{II}]$$

The term reduced, designated by the subscript "r", means that the resulting mass and stiffness matrices, $[K_r]$ & $[M_r]$, are of smaller dimension than the original matrix. Although this transformation matrix reduces the size of the component model, it does not assemble the individual substructure models. There is a second transformation matrix that synthesizes the substructures to produce the total system by enforcing the compatibility and equilibrium of the interface coordinates as follows:

$$\{X_I^1\} = \{X_I^2\} \tag{15a}$$
$$\{F_I^1\} = -\{F_I^2\} \tag{15b}$$

The compatibility of interface coordinates denoted by Eq.(15a) implies that the displacement at the interface of structure 1 equals the displacement at the interface of structure 2. Likewise, the equilibrium of interface forces denoted by Eq.(15b) implies that the sum of the forces at the interface are equal but in acting in opposite directions. Since the static constraint modes are independent of the fixed interface normal modes, the transformation matrix, or $[T_2]$, takes the following form:

$$\begin{Bmatrix} p_O^1 \\ p_I^1 \\ p_O^2 \\ p_I^2 \end{Bmatrix} = \begin{bmatrix} [I] & [0] & [0] \\ [0] & [0] & [I] \\ [0] & [I] & [0] \\ [0] & [0] & [I] \end{bmatrix} \begin{Bmatrix} p_O^1 \\ p_O^2 \\ p_I^1 \end{Bmatrix} = \begin{Bmatrix} p_O^1 \\ p_I^1 \\ p_O^2 \\ p_I^2 \end{Bmatrix} = [T_2] \begin{Bmatrix} p_O^1 \\ p_O^2 \\ p_I^1 \end{Bmatrix} \qquad (16)$$

where superscript "1" refers to substructure 1 (i.e., mast), and superscript "2" refers to substructure 2 (i.e., antenna). In Eq.(16), p_O represents the physical internal coordinates, and p_I represents the physical interface coordinates.

The system model is obtained from an uncoupled mass and stiffness matrix. These uncoupled mass and stiffness matrices are themselves formed from the reduced mass and stiffness matrices from each substructure as follows:

$$[M_u] = \begin{bmatrix} M_r^1 & 0 \\ 0 & M_r^2 \end{bmatrix} \qquad [K_u] = \begin{bmatrix} K_r^1 & 0 \\ 0 & K_r^2 \end{bmatrix} \qquad (17a,b)$$

where the subscript "u" denotes "uncoupled."

The coupled system mass and stiffness matrices are obtained by pre-multiplying the uncoupled mass and stiffness matrices in Eq. (17a,b) by the transpose of the transformation matrix in Eq. (16) and then post-multiplying the uncoupled mass and stiffness matrices by the transformation matrix.

$$[M_s] = [T_2]^T [M_u] [T_2] \qquad [K_s] = [T_2]^T [K_u] [T_2] \qquad (18a,b)$$

where the subscript "s" denotes "system."

The resulting coupled system mass and stiffness matrices are of the form:

$$[M_s] = \begin{bmatrix} M^1_{KK} & 0 & M^1_{KI} \\ 0 & M^2_{KK} & M^2_{KI} \\ M^1_{IK} & M^2_{IK} & M_{II} \end{bmatrix} \qquad [K_s] = \begin{bmatrix} K^1_{KK} & 0 & 0 \\ 0 & K^2_{KK} & 0 \\ 0 & 0 & K_{II} \end{bmatrix} \qquad (19a,b)$$

where "I" represents the interface coordinates, and "K" represents the kept internal coordinates [4]. The respective partitions of the system mass and stiffness matrices are expressed as follows:

$$M^1_{KK} = [I^1_{KK}]$$
$$M^2_{KK} = [I^2_{KK}]$$
$$M^1_{KI} = M^{1\,T}_{IK} = [\Psi^{X1^T}(M^1_{OO}(-K^{-1}_{OO}K_{O1})^1 + M^1_{O1})]$$
$$M^2_{KI} = M^{2\,T}_{IK} = [\Psi^{X2^T}(M^2_{OO}(-K^{-1}_{OO}K_{O1})^2 + M^2_{O1})]$$
$$M_{II} = [(-K^{-1}_{OO}K_{O1})^{1^T}(M^1_{OO}(-K^{-1}_{OO}K_{O1})^1 + M^1_{O1}) + M^1_{IO}(-K^{-1}_{OO}K_{O1})^1 + M^1_{II} + \ldots$$
$$(-K^{-1}_{OO}K_{O1})^{2^T}(M^2_{OO}(-K^{-1}_{OO}K_{O1})^2 + M^2_{O1}) + M^2_{IO}(-K^{-1}_{OO}K_{O1})^2 + M^2_{II}]$$

$$K^1_{KK} = [\Lambda^{\,1}_{KK}]$$
$$K^2_{KK} = [\Lambda^{\,2}_{KK}]$$
$$K_{II} = [K^1_{II} - K^1_{IO}K^{-1\,1}_{OO}K^1_{OI} + K^2_{II} - K^2_{IO}K^{-1\,2}_{OO}K^2_{OI}]$$

There are a number of advantages to the Craig-Bampton component mode representation. The first, which is especially beneficial to the analysis of the mast/antenna system, is that the reduced DOF system contain the interface DOF explicitly. This makes it very easy to couple mast and antenna substructures. In the figure on the following page is an illustration of the mast/antenna system used for the examples in this report. Along

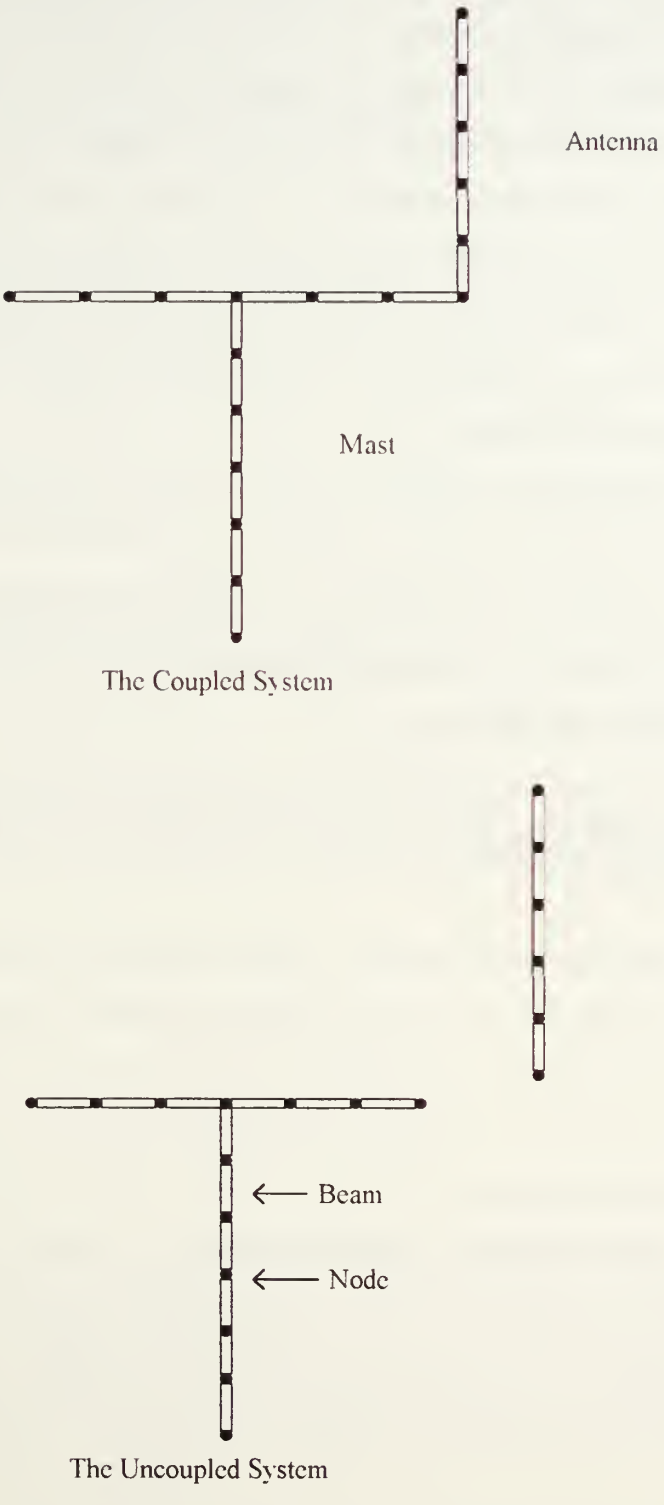

Figure 1: The Coupled & Uncoupled Mast and Antenna Systems

the length of the cross bar are various node positions. These node positions serve to connect the beams that represent the cross bar, and can also serve as nodes to connect various antennae to the crossbar. By specifying different "connection coordinates" (i.e., the "I" coordinates), and with separate mast and antenna data files contained in the library, the engineer can quickly couple various antennae with the mast and rapidly determine dynamic response. Should the location of the antenna placement not be suitable, the engineer can specify a new set of interface coordinates along the cross bar, plug in the antenna at the new location, and rapidly calculate a system from which a new dynamic response can be calculated.

Because of these advantages, and because the Craig-Bampton component mode representation tends to result in accurate system frequencies, as will be shown, this is a widely used method. Additionally, the NASTRAN superelement scheme uses the Craig-Bampton component mode representation with minor extensions as a solution path to the dynamic response problem.

B. CRAIG-CHANG AND MACNEAL RESIDUAL FLEXIBILITY FORMULATIONS

The Craig-Chang and MacNeal residual flexibility formulations will now be discussed. Due to the similarity in the methods, the Craig-Chang procedure will be presented first, and the modification of this method to produce the final system of equations of the MacNeal method will be discussed subsequently. While the Craig-Bampton representation uses a combination of static constraint modes and fixed interface normal modes, the Craig-Chang residual flexibility formulation combines free interface mode shapes with residual flexibility shapes; thus the name: residual flexibility method. The transformation matrix which is used to reduce the component mass and stiffness matrices contains columns of the retained or kept free interface normal modes and residual flexibility modes.

The transformation matrix, or $[T_1]$, is shown as follows:

$$\begin{Bmatrix} x_O \\ x_I \end{Bmatrix} = \begin{bmatrix} \Phi^{\sim}_{KO} & \Psi_{OI} \\ \Phi^{\sim}_{KI} & \Psi_{II} \end{bmatrix} \begin{Bmatrix} q_O \\ q_I \end{Bmatrix} = [T_1] \begin{Bmatrix} q_O \\ q_I \end{Bmatrix} \tag{20}$$

In the same way that we reduced the Craig-Bampton components, we reduce the Craig-Chang components except now using the transformation matrix of Eq (20). Again, each component has its own transformation matrix. A reduction in component matrix size is achieved by retaining fewer than the total number of free interface normal modes. The number of residual flexibility mode shapes is fixed, and equals the number of interface degrees of freedom.

Just like the Craig-Bampton formulation, the purpose of the transformation matrix is to reduced the respective component models before synthesis of the system model. This transformation matrix does not synthesize the substructures. Another transformation matrix is employed to synthesize the substructures. As in the Craig-Bampton formulation, this second transformation matrix results from satisfying compatibility and equilibrium equations:

$$\{x_I^{\,1}\} = \{x_I^{\,2}\} \tag{21a}$$

$$\{F_I^{\,1}\} = -\{F_I^{\,2}\} \tag{21b}$$

Unlike the Craig-Bampton component mode representation where the static constraint modes are independent of the fixed interface normal modes, the residual flexibility modes are dependent upon the free interface normal modes, and a simple boolean matrix will not synthesize the substructures. Although not derived in this report, the second transformation matrix, or $[T_2]$, is as follows:

$$[T_2] = \begin{bmatrix} -k_1\Phi^1_{KI} & k_1\Phi^2_{KI} \\ k_1\Phi^1_{KI} & -k_1\Phi^2_{KI} \\ [I] & [0] \\ [0] & [I] \end{bmatrix} \tag{22}$$

where $k_1 = (\Psi^1_{II} + \Psi^2_{II})^{-1}$.

As in the Craig-Bampton procedure, the uncoupled mass and stiffness matrices are assembled from the reduced component mass and stiffness matrices.

$$[M_u] = \begin{bmatrix} M^1_{DD} & 0 & 0 & 0 \\ 0 & M^2_{DD} & 0 & 0 \\ 0 & 0 & I^1_{KK} & 0 \\ 0 & 0 & 0 & I^2_{KK} \end{bmatrix} \qquad [K_u] = \begin{bmatrix} K^1_{DD} & 0 & 0 & 0 \\ 0 & K^2_{DD} & 0 & 0 \\ 0 & 0 & \Lambda^1_{KK} & 0 \\ 0 & 0 & 0 & \Lambda^2_{KK} \end{bmatrix} \tag{23a,b}$$

By pre- and post-multiplying both the uncoupled mass matrix represented by Eq. (23a) and the uncoupled stiffness matrix represented by Eq. (23b) by $[T_2]^T$ and $[T_2]$ respectively, in the same manner that the Craig-Bampton component mode representation was coupled, the system equations of motion are obtained as follows:

$$[M_s] = \begin{bmatrix} M_{11} & M_{12} \\ M_{21} & M_{22} \end{bmatrix} \qquad [K_s] = \begin{bmatrix} K_{11} & K_{12} \\ K_{21} & K_{22} \end{bmatrix} \tag{24a,b}$$

The partitions of the system mass and stiffness matrices represented by Eq.(24a,b) are given as follows:

$$M_{11} = \left[I^1_{KK} + \Phi^{1^T}_{IK} m_1 \Phi^1_{IK}\right] \qquad K_{11} = \left[\Lambda^1_{KK} + \Phi^{1^T}_{IK} k_1 \Phi^1_{IK}\right]$$

$$M_{12} = M^T_{21} = \left[-\Phi^{1^T}_{IK} m_1 \Phi^2_{IK}\right] \qquad K_{12} = K^T_{21} = \left[-\Phi^{1^T}_{IK} k_1 \Phi^2_{IK}\right]$$

$$M_{22} = \left[I^2_{KK} + \Phi^{2^T}_{IK} m_1 \Phi^2_{IK}\right] \qquad K_{22} = \left[\Lambda^2_{KK} + \Phi^{2^T}_{IK} k_1 \Phi^2_{IK}\right]$$

$$M_{11} = \left[I^1_{KK} + \Phi^{1^T}_{IK} m_1 \Phi^1_{IK} \right] \qquad K_{11} = \left[\Lambda^{\ 1}_{KK} + \Phi^{1^T}_{IK} k_1 \Phi^1_{IK} \right]$$

$$M_{12} = M^T_{21} = \left[-\Phi^{1^T}_{IK} m_1 \Phi^2_{IK} \right] \qquad K_{12} = K^T_{21} = \left[-\Phi^{1^T}_{IK} k_1 \Phi^2_{IK} \right]$$

$$M_{22} = \left[I^2_{KK} + \Phi^{2^T}_{IK} m_1 \Phi^2_{IK} \right] \qquad K_{22} = \left[\Lambda^{\ 2}_{KK} + \Phi^{2^T}_{IK} k_1 \Phi^2_{IK} \right]$$

where $m_1 = k_1 (M^1_{DD} + M^2_{DD}) k_1$ [5]. The inertia due to high order free interface normal modes is represented by "m_1."

As stated in the beginning of this section, the MacNeal component mode representation would be presented By neglecting the inertia due to high-order free-interface normal modes, (i.e. "m_1"), one obtains the MacNeal mass and stiffness matrices as follows:

$$M_{11} = \left[I^1_{KK} \right] \qquad K_{11} = \left[\Lambda^{\ 1}_{KK} + \Phi^{1^T}_{IK} k_1 \Phi^1_{IK} \right]$$

$$M_{12} = M^1_{21} = [0] \qquad K_{12} = K^T_{21} = \left[-\Phi^{1^T}_{IK} k_1 \Phi^2_{IK} \right]$$

$$M_{22} = \left[I^2_{KK} \right] \qquad K_{22} = \left[\Lambda^{\ 2}_{KK} + \Phi^{2^T}_{IK} k_1 \Phi^2_{IK} \right]$$

As will be demonstrated through the examples, the effect of neglecting "m_1" is important when predicting the higher frequencies [6]. The MacNeal representation is accurate in the lower and mid frequency range, but less accurate in the higher frequency range.

Just like the Craig-Bampton component mode representations there are several advantages to both residual flexibility methods. By analyzing both the Craig-Chang and MacNeal system mass and stiffness matrices, one can see that the final system coordinates are just the free interface normal mode coordinates from each substructure. This resulted from the operations that were conducted in forming the system mass and stiffness matrices. Additionally, since the residual flexibility modes account for the static flexibility of all modes, the methods are statically exact. The procedure is applicable to the mast and antenna problem. Since the connection coordinates are not explicitly retained, this

connection points, and the residual flexibility method does not retain the connection coordinates explicitly, a reduction in compute times result, an advantage not found in other substructure coupling procedures.

IV. NUMERICAL VERIFICATION

In this section some numerical examples which demonstrate the use of the three component mode synthesis procedures will be presented. A "mock-up" mast and antenna system consisting of 17 elements was assembled using a standard finite element procedure and all three component mode synthesis procedures. Although the mast/antenna system that is used in the examples is modeled with just a few elements, the resulting models are large enough to allow the effects of mode truncation to be assessed. Again, it is not the intent of this report to solve a base excitation problem on a realistic mast and antenna model, but rather to demonstrate how CMS can be used when performing dynamic analyses for design purposes.

Example 1 compares natural frequency calculations for the total mast/antenna system as computed using the three CMS formulations as well as using a standard FE procedure. Tables 1-3 contain the results of this comparison. In the tables, each row contains the estimate of a mode frequency. The first column contains the mast/antenna system natural frequency estimates as calculated using the standard FE procedure, and serves as the reference value against which the CMS natural frequency estimates are to be compared. Columns 2 through 4 contain the analogous natural frequency estimates and percent error, as calculated from the mast/antenna system model synthesized using each of the three CMS procedures. Also included in the column headings are floating point operations (FLOPS) counts which provide a measure of the number of calculations required to assemble the mast/antenna system and calculate the natural frequencies and mode shapes.

Table 1 presents the system frequency comparison where 18% of the available mast modes are retained, and 22% of the available antenna modes are retained. Table 2 repeats the calculations with 42% of the available mast modes retained and 39% of the available antenna modes retained, and Table 3 repeats the calculations with 79% of the available

mast modes retained and 67% of the available antenna modes retained. Note that each subsequent table presents comparisons for an increasing number of mode frequencies due to the fact that an increase in the number of retained component modes makes possible an increase in the number of system modes which may be calculated.

Note that in the FEM model, the FLOPS count stays fixed at slightly over $2 \cdot 10^6$. This is a rather small number as the model is a small model when compared to one that a design engineer would generate for analysis of an actual mast/antenna assembly. It is noteworthy to state that in this particular model, $0.7 \cdot 10^6$ FLOPS were expended in computing the combination of fixed interface normal modes and static constraint modes using the Craig-Bampton procedure. Additionally, $0.8 \cdot 10^6$ FLOPS were expended in computing the free interface normal modes using the Craig-Chang and MacNeal procedures. Theoretically, once the various vibrational modes have been found, they need not be calculated again. Note also that in all three models, these figures comprise a significant portion of the total FLOPS.

From Tables 1 through 3, it is seen that all three methods produce excellent frequency predictions. All three methods demonstrate sudden increases in frequency error above a certain mode. This reveals the extent to which the retained component modes accurately represent the dynamics of the synthesized mast/antenna system. In the MacNeal procedure, the percentage error exceeded 100% when calculating the highest mode. This error in predicting the highest frequency mode could possibly be attributed to neglecting the inertia due to high-order free interface normal modes. Note that by neglecting the inertia, that the accuracy in predicting natural frequencies is only effected at the last few modes.

As stated in the previous paragraph, all three methods produced excellent results in predicting natural frequencies, but with less cost in terms of number of computations as compared to the standard FE calculation. The Craig-Chang procedure in general provided the greatest number of natural frequencies with error less than or equal to 0.1% (in Hz) (see figure 2). However, the Craig-Bampton procedure yielded the same number of

frequencies with error less than or equal to 0.1% as the Craig-Chang procedure when retaining a large of number of component modes, but at a slightly more cost than the Craig-Chang procedure.

Table 1. Coupled System Natural Frequency Comparison
Percent of Available Mast Modes Retained: 18%
Percent of Available Antenna Modes Retained: 22%

Mode No.	Standard Finite Element (2.05E+06 FLOPS)	Craig-Bampton (7.72E+05 FLOPS)		Craig-Chang (1.17E+06 FLOPS)		MacNeal (1.06E+06 FLOPS)	
	Freq. (Hz)	Freq. (Hz)	Error (%)	Freq. (Hz)	Error (%)	Freq. (Hz)	Error (%)
1	6.885	6.885	0.002	6.885	0.000	6.887	0.019
2	10.396	10.398	0.019	10.396	0.002	10.398	0.020
3	13.301	13.301	0.002	13.301	0.000	13.301	0.000
4	19.102	19.104	0.012	19.102	0.002	19.102	0.002
5	47.257	47.260	0.007	47.260	0.007	47.403	0.309
6	69.884	70.040	0.224	69.893	0.013	70.155	0.388
7	83.502	83.504	0.003	83.502	0.000	83.503	0.000
8	121.024	134.053	10.765	121.372	0.287	121.441	0.344
9	122.115	184.492	51.080	143.508	17.518	238.807	95.559
10	135.967	303.331	>100.00	222.630	63.738	341.199	>100.00

Notes: The column "Standard Finite Element" contains the mode frequencies for the mast/antenna system assembled using a standard finite element approach. The corresponding mode frequency estimates for the three synthesis methods are shown in the three columns to the right. The Floating Point Operations (FLOPS) required for each synthesis method and the finite element calculation are shown. Retained mode percentages are rounded to the nearest integer for clarity.

Table 2. Coupled System Natural Frequency Comparison
Percent of Available Mast Modes Retained: 42%
Percent of Available Antenna Modes Retained: 39%

Mode No.	Standard Finite Element (2.05E+06 FLOPS)	Craig-Bampton (8.63E+05 FLOPS)		Craig-Chang (1.23E+06 FLOPS)		MacNeal (1.15E+06 FLOPS)	
	Freq. (Hz)	Freq. (Hz)	Error (%)	Freq. (Hz)	Error (%)	Freq. (Hz)	Error (%)
1	6.885	6.885	0.000	6.885	0.001	6.885	0.001
2	10.396	10.396	0.000	10.396	0.002	10.396	0.002
3	13.301	13.301	0.001	13.301	0.000	13.301	0.000
4	19.102	19.092	0.050	19.102	0.002	19.102	0.002
5	47.257	47.257	0.000	47.257	0.001	47.260	0.007
6	69.884	69.886	0.003	69.883	0.001	69.886	0.002
7	83.502	83.503	0.000	83.502	0.000	83.502	0.000
8	121.024	121.058	0.028	121.027	0.002	121.028	0.003
9	122.115	122.197	0.067	122.118	0.002	122.119	0.003
10	135.967	135.971	0.003	135.964	0.002	136.021	0.040
--							
19	462.776	463.860	0.234	463.361	0.127	468.640	1.267
20	537.237	537.239	0.000	537.237	0.000	537.238	0.000
21	647.348	706.684	9.166	648.220	0.135	649.499	0.332
22	692.643	735.918	6.248	721.256	4.131	746.016	7.706
23	733.509	934.920	27.459	738.706	0.709	900.717	22.796
24	756.314	1256.376	66.118	1019.930	34.855	2453.914	>100.00

Notes: The column "Standard Finite Element" contains the mode frequencies for the mast/antenna system assembled using a standard finite element approach. The corresponding mode frequency estimates for the three synthesis methods are shown in the three columns to the right. The Floating Point Operations (FLOPS) required for each synthesis method and the finite element calculation are shown. Retained mode percentages are rounded to the nearest integer for clarity. Modes 11 through 18 excluded to conserve space.

Table 3. Coupled System Natural Frequency Comparison
Percent of Available Mast Modes Retained: 79%
Percent of Available Antenna Modes Retained: 67%

Mode No.	Standard Finite Element (2.05E+06 FLOPS)	Craig-Bampton (1.82E+06 FLOPS)		Craig-Chang (1.80E+06 FLOPS)		MacNeal (1.66E+06 FLOPS)	
	Freq. (Hz)	Freq. (Hz)	Error (%)	Freq. (Hz)	Error (%)	Freq. (Hz)	Error (%)
1	6.885	6.885	0.000	6.885	0.001	6.885	0.001
2	10.396	10.396	0.000	10.396	0.002	10.396	0.002
3	13.301	13.301	0.001	13.301	0.000	13.301	0.000
4	19.102	19.092	0.050	19.102	0.002	19.102	0.002
5	47.257	47.257	0.000	47.257	0.001	47.258	0.003
--							
28	977.426	978.347	0.094	977.447	0.002	978.075	0.066
29	1022.223	1022.255	0.003	1022.234	0.001	1022.294	0.007
30	1098.507	1098.592	0.008	1098.893	0.035	1108.635	0.922
31	1267.414	1267.416	0.000	1267.445	0.002	1267.854	0.035
32	1306.822	1306.373	0.034	1306.876	0.004	1307.009	0.014
33	1415.797	1418.637	0.201	1420.494	0.332	1468.806	3.744
34	1477.522	1477.863	0.023	1477.798	0.019	1499.859	1.512
35	1538.404	1539.828	0.093	1547.072	0.564	1578.170	2.585
36	1656.532	1659.662	0.189	1659.529	0.181	1684.335	1.678
37	1671.847	2009.052	20.170	1785.483	6.797	2623.856	56.944
38	1885.441	2275.957	20.712	2040.943	8.248	7736.296	>100.00

Notes: The column "Standard Finite Element" contains the mode frequencies for the mast/antenna system assembled using a standard finite element approach. The corresponding mode frequency estimates for the three synthesis methods are shown in the three columns to the right. The Floating Point Operations (FLOPS) required for each synthesis method and the finite element calculation are shown. Retained mode percentages are rounded to the nearest integer for clarity. Modes 6 through 27 excluded to conserve space.

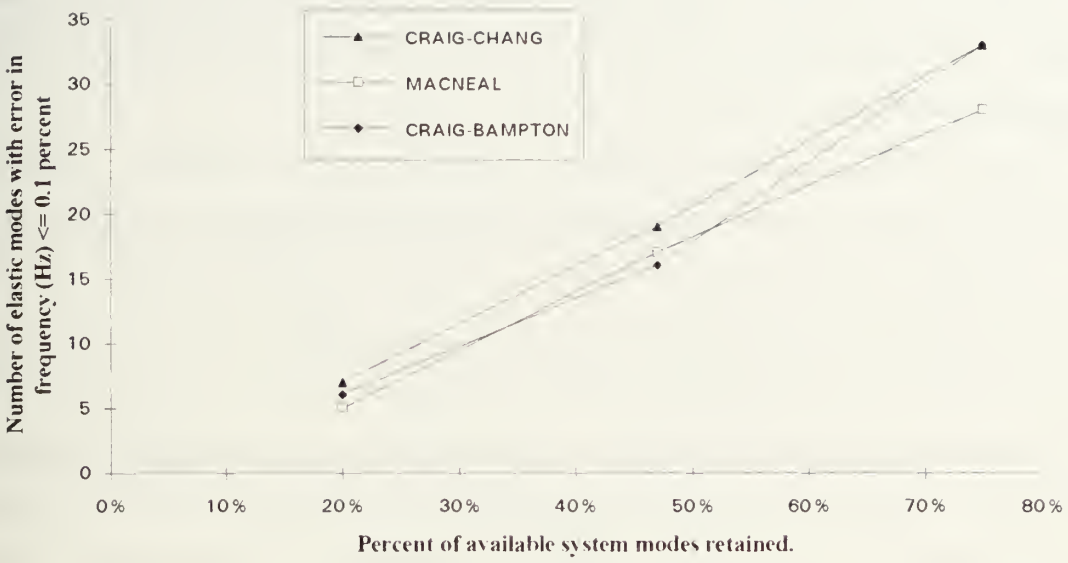

Figure 2: Comparison of CMS methods with frequency (Hz) error of <= 0.1 percent for mast/antenna system

V. BASE EXCITATION FORMULATIONS

In the previous section, the natural frequencies of the mast and antenna system were calculated for increasing number of retained component modes. Natural frequencies and mode shapes are important modal parameters and are fundamental in solving for the forced response of a system. As demonstrated in the previous section, accurate natural frequencies of a system can be obtained using CMS at a cost less than that associated with standard FE modeling.

In this section, two base excitation formulations will be presented. The first formulation requires the knowledge of the acceleration of the mast base coordinates (i.e. the coordinates where the mast and ship are coupled) as a function of time. In other words, the formulation requires that the acceleration time history of the base coordinates be known. The second formulation requires the knowledge of the displacement of the base coordinates as a function of time, or the displacement time history of the base coordinates. Using both formulations, numerical convergence assessments will be made, and the benefits that CMS has to offer the mast/antenna design process will be demonstrated.

A. BASE EXCITATION FROM PRESCRIBED ACCELERATION

Once the FE program has numerically assembled the mast mass and stiffness matrices, and the acceleration of the base coordinates are specified as a function of time, the base excitation problem can be derived from the following equation of motion:

$$\begin{bmatrix} M_{OO} & M_{OB} \\ M_{BO} & M_{BB} \end{bmatrix} \begin{Bmatrix} \ddot{x}_O \\ \ddot{x}_B \end{Bmatrix} + \begin{bmatrix} K_{OO} & K_{OB} \\ K_{BO} & K_{BB} \end{bmatrix} \begin{Bmatrix} x_O \\ x_B \end{Bmatrix} = \begin{Bmatrix} F_O \\ 0 \end{Bmatrix} \tag{25}$$

where subscript "O" represents the interior coordinates, and subscript "B" represents the base coordinates.

Solving the top row of equations in Eq (25) the following is obtained:

$$M_{OO}\ddot{x}_O + M_{OB}\ddot{x}_B + K_{OO}x_O + K_{OB}x_B = F_O \tag{26}$$

Since the acceleration of the base is prescribed, the base acceleration term will be moved to the right hand of the equals sign to obtain the following:

$$M_{OO}\ddot{x}_O + K_{OO}x_O + K_{OB}x_B = F_O - M_{OB}\ddot{x}_B \tag{27}$$

From the bottom row, the following equation is obtained:

$$M_{BO}\ddot{x}_O + M_{BB}\ddot{x}_B + K_{BO}x_B + K_{BB}x_B = 0 \tag{28}$$

From Eq. (28), the following relation is obtained for the base displacement:

$$x_B = -K_{BB}^{-1}\left[M_{BO}\ddot{x}_O + M_{BB}\ddot{x}_B + K_{BO}x_O\right] \tag{29}$$

Equation (29) is now substituted into Eq. (27), and after simplifying, the following equation of motion in terms of the interior coordinates is obtained as follows:

$$\left[M_{OO} - K_{OB}K_{BB}^{-1}M_{BO}\right]\ddot{x}_O + \left[K_{OO} - K_{OB}K_{BB}^{-1}K_{BO}\right]x_O = F_O + \left[K_{OB}K_{BB}^{-1}M_{BB} - M_{OB}\right]\ddot{x}_B \tag{30}$$

Equation (30) is the system equation of motion of the internal coordinates in terms of the prescribed base acceleration.

The physical coordinates are transformed into modal coordinates by the following relation:

$$\{X_o\} = [\Phi^N] \cdot \{q_o\} \tag{31}$$

where $\{X_o\}$ represents the vector of physical internal coordinates, $\{q_o\}$ represents the vector of modal internal coordinates, and $[\Phi^N]$ represents the matrix of unity modal mass free interface normal modes.

Equation (30) is then pre-multiplied by the transpose of the matrix of normal modes to obtain the following modal system of equations:

$$[I]\{\ddot{q}_o\} + [\Lambda]\{q_o\} = \{F\} \tag{32}$$

where $\{\ddot{q}_o\}$ represents the vector of modal accelerations and $\{F\}$ represents the vector of modal forces.

The relation in Eq. (32) is solved using standard modal decomposition techniques. Once the modal response is obtained, Eq. (31) is used to obtain the response in physical coordinates.

In what follows, the relation in Eq. (30) is used in conjunction with a standard FE model of the total mast/antenna system to perform the prescribed base acceleration dynamic analysis. This analysis serves as the reference against which the results of various CMS formulations are to be compared. In each CMS formulation, Eq. (30) is used to define the mast component model, as only the mast has prescribed base accelerations.

The acceleration at the base is a prescribed harmonic input. The base acceleration is taken as:

$$\{\ddot{x}_B\} = -\omega^2 \{X_B\} \sin(\omega t) \tag{33}$$

where "ω" represents the forcing frequency expressed in rad/sec, and $\{X_B\}$ represents the vector of amplitudes of the base displacement expressed in inches.

In the following section, two numerical examples are provided. It is the intent of the examples to:

(1) compare the results obtained from the three CMS formulations

(2) and demonstrate the benefits of using CMS versus standard FE modeling when solving base excitation problems.

1. TIP DEFLECTION CALCULATION

On the following page is a diagram of the mast and antenna system being subjected to base excitation. The excitation was performed at two different and arbitrarily selected frequencies. The first frequency was at 8.95 Hz. This frequency falls between mode 1 and mode 2 of the total mast/antenna system. The second frequency was between mode 9 and mode 10 at 219 Hz. The wide spread in the frequencies was intended to demonstrate that many more modes need to be retained when calculating the response to higher frequency excitation as compared with lower frequency excitations. In this example, the antenna tip deflection was calculated using the standard FE procedure and the three CMS procedures. The percent error in antenna tip deflection was plotted versus the percent of available component modes retained (see figures 4-7). The calculations were performed twice. In the first calculation, mast modes were truncated while retaining all of the available antenna modes, and antenna modes were truncated in the second calculation while retaining all of the available mast modes. When the mast was subjected to the forced input at the lower frequency the Craig-Bampton and Craig-Chang procedure yielded results which converged more rapidly to the exact answer than the MacNeal procedure.

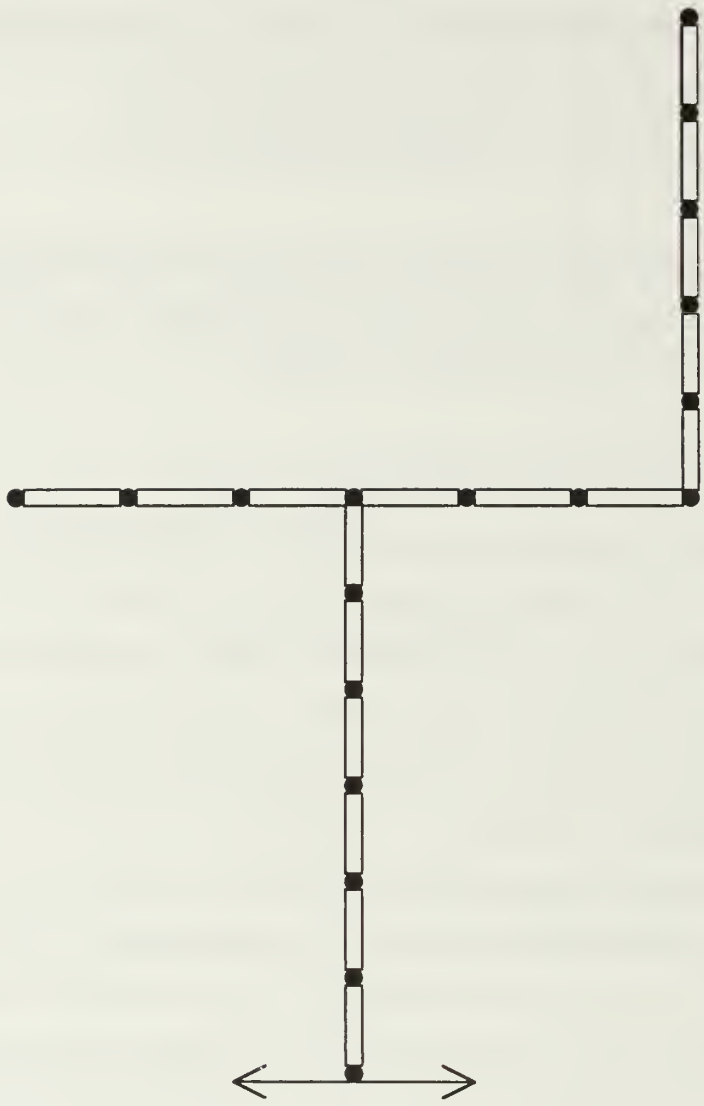

Figure 3: The Coupled Mast and Antenna Subjected to Base Excitation at 8.95 Hz

Although, hard to determine from figures 4 and 5, the Craig-Bampton procedure yielded the best results using fewer modes than the Craig-Chang procedure in both the mast truncation and antenna truncation runs. When 20% of the available mast modes were used, all three procedures predicted a tip deflection measurement that was within 0.05% of the "exact" value (the "exact" value was calculated using the standard FE procedure). This accurate assessment was obtained at a cost of 60% of the number of calculations that were required of the FE solution. The error obtained when 20% of the available mast modes were retained was significantly small. Since all of the vibrational mode shapes were obtained in this calculation (i.e. fixed interface normal modes, free interface normal modes, static constraint modes, and residual flexibility modes), future assessments which retain more mast modes would come at an even lesser cost than the initial assessment.

When the mast was subjected to the higher forcing frequency, all three methods converged more slowly as compared to the lower forcing frequency when truncating both mast modes and antenna modes (see figures 6 and 7). Since the forcing frequency was higher, more modes needed to be retained in order to obtain accurate results. From the results of the tip deflection calculations, it appears that the combination of fixed interface normal modes and static constraint modes have led to the higher rate of convergence using the Craig-Bampton procedure. However, the results obtained using the Craig-Chang procedure compared quite well with the results obtained using the Craig Bampton method

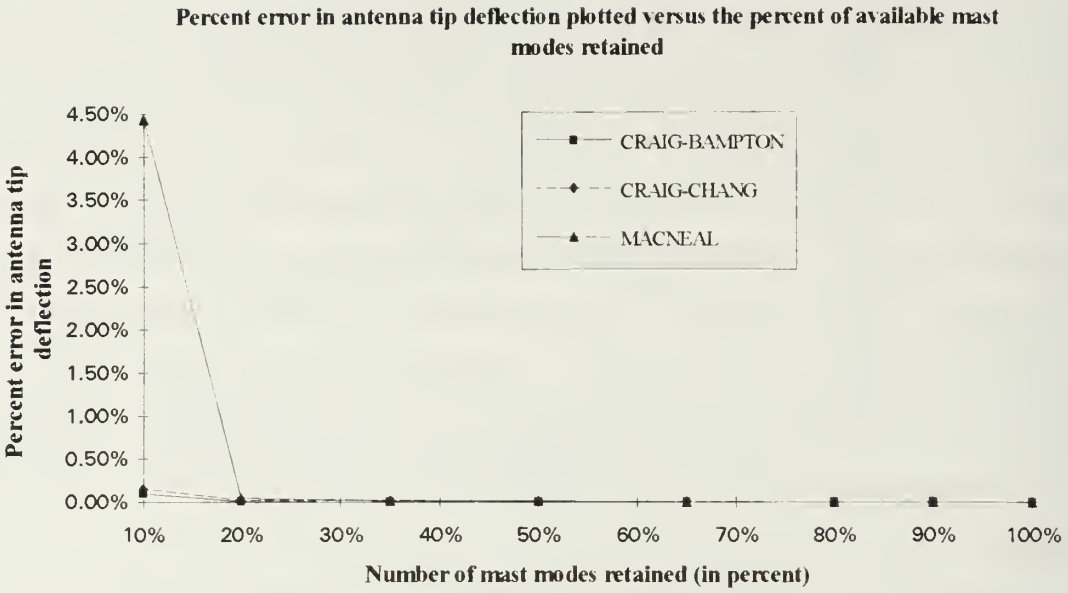

Figure 4: Percent error in antenna tip deflection plotted versus the percent of available mast modes retained. (Forcing frequency: 8.95 Hz)

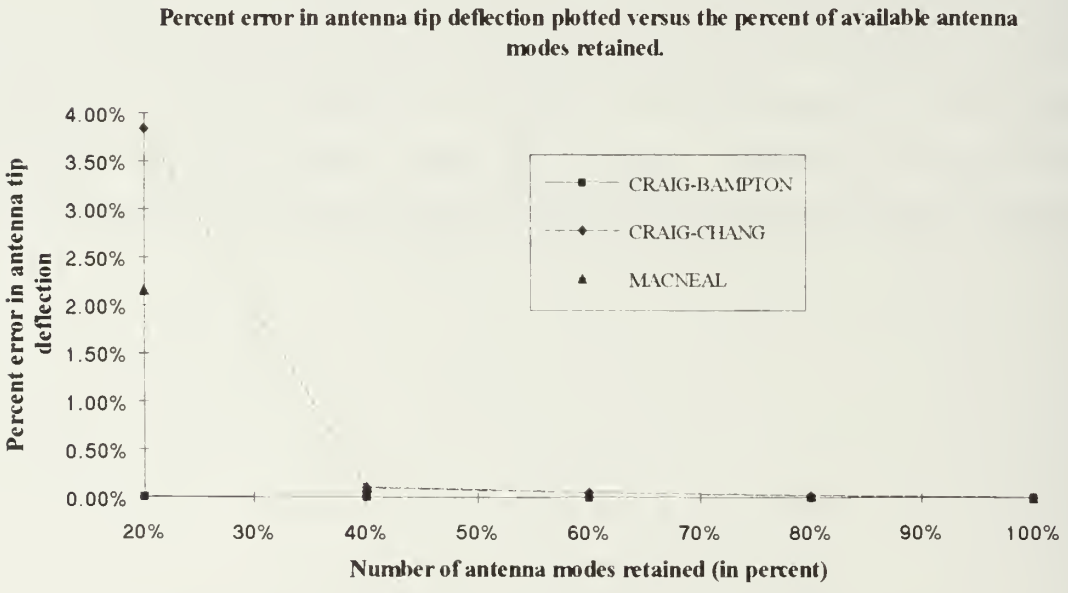

Figure 5: Percent error in antenna tip deflection plotted versus the percent of available antenna modes retained. (Forcing Frequency: 8.95 Hz)

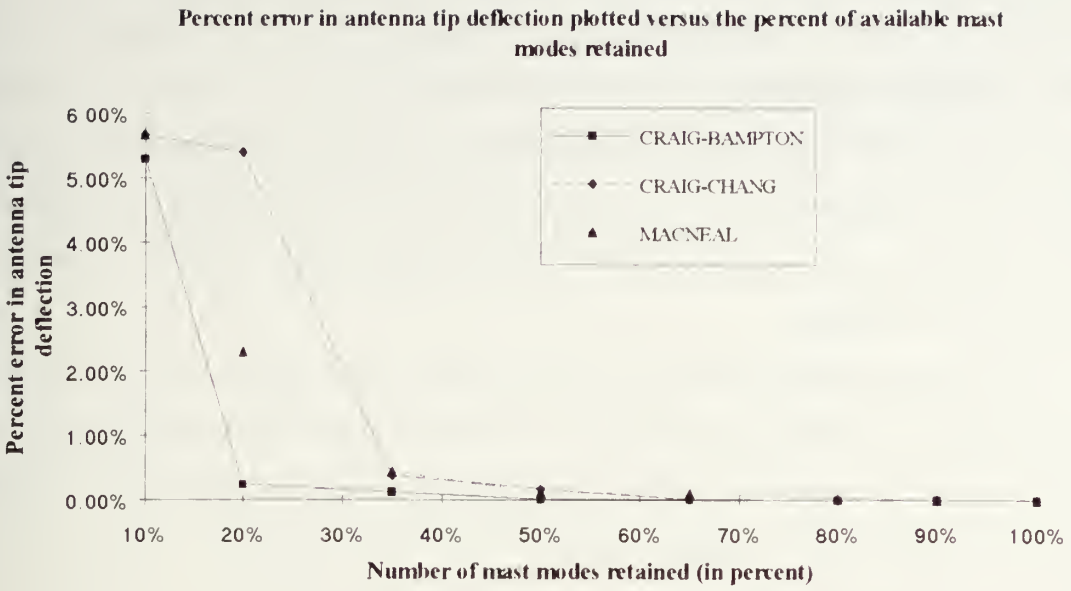

Figure 6: Percent error in antenna tip deflection plotted versus the percent of available mast modes retained. (Forcing Frequency: 219 Hz)

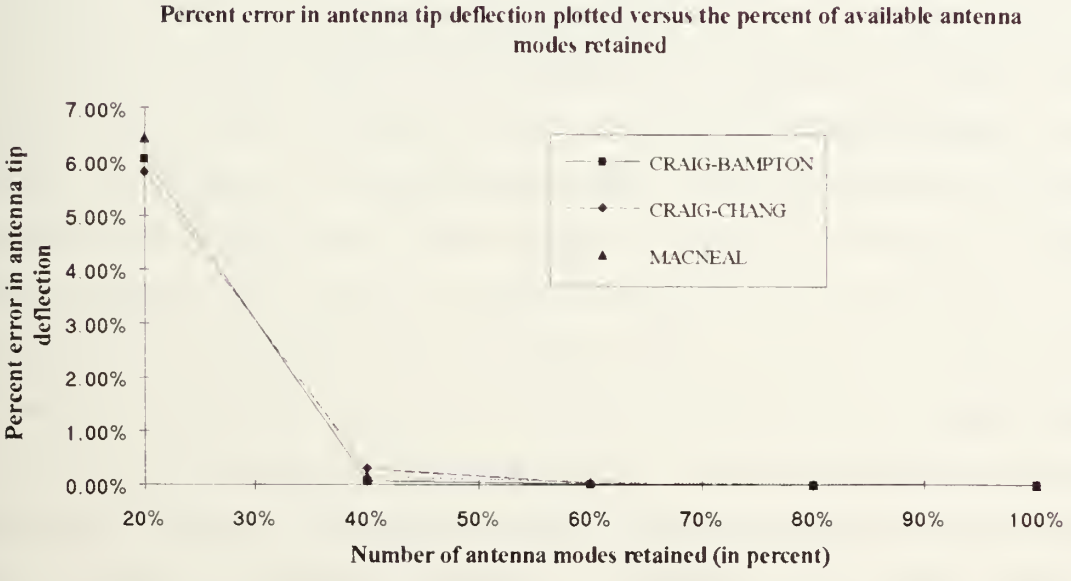

Figure 7: Percent error in antenna tip deflection plotted versus the percent of available antenna modes retained. (Forcing Frequency: 219 Hz)

2. MOMENT AND SHEAR CALCULATION

In order to assess structural survivability, accurate prediction of the internal stresses in the antenna and the antenna/mast interface must be calculated. Therefore, this section demonstrates the calculation of the internal peak dynamic bending moments and shear loads in the antenna.

The moment and shear calculations were calculated using the three CMS procedures and the results are compared in the figures. The percent error in moment and shear were plotted versus the percent of available mast modes retained and percent of available antenna modes retained. Again, the same two forcing frequencies used in the tip deflection calculation are used here in the moment and shear calculations; specifically 8.95 and 219 Hz.

The results obtained when calculating the shear and moment at the mast/antenna connection mirror the results of the tip deflection calculations (see figures 8-15). Again, the Craig-Bampton procedure yielded results that converged more quickly to the "exact" answer (provided by standard FE calculations) than the other methods. However, the results obtained using the Craig-Chang procedure were quite similar to those obtained using the Craig-Bampton method. Despite a large initial error produced by the MacNeal method as compared to the other two methods, nearly "exact" solutions were obtained at a cost much less than using standard FE calculation procedures. If the moment and shear at the mast/antenna interface exceeded an appropriate failure criteria, the antenna can be easily relocated from the end node to another node along the cross bar by redefining the connection coordinates of the mast. New moment and shear calculations would be made until an acceptable response obtained. Redefining the connection coordinates, synthesizing the new structure, and calculating the response is much more convenient and computationally efficient than reassembling the mast and antenna system, which would be required using standard FE procedures.

When the mast and antenna system were subjected to the forced input at the higher forcing frequency, the rate of convergence was again much slower than that which was obtained at the lower excitation frequency. However, all methods yield accurate results at a computational cost less than using the standard FE procedure with the higher forcing frequency.

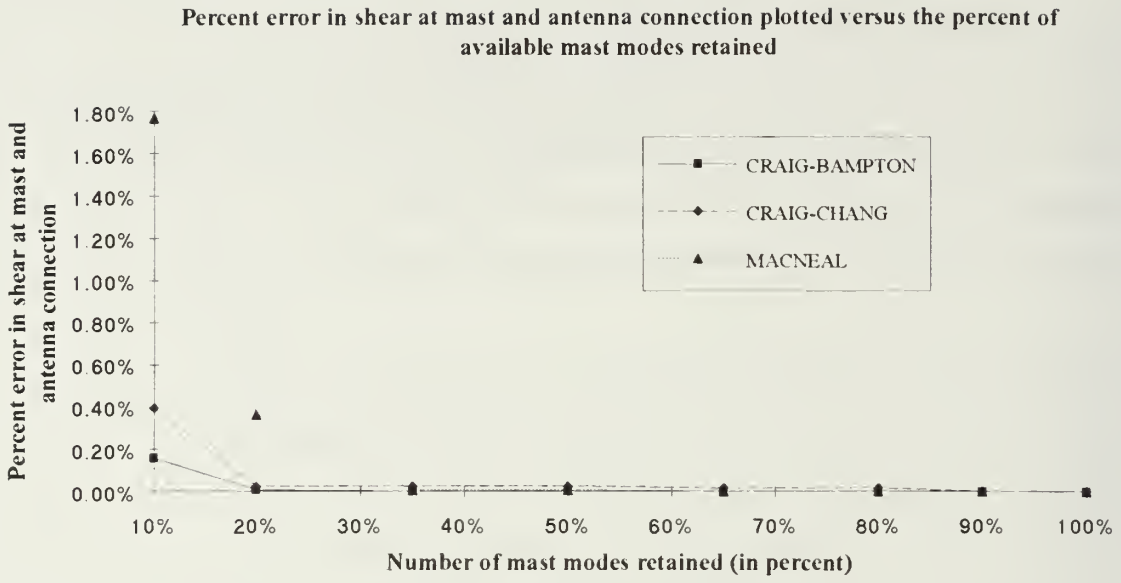

Figure 8: Percent error in shear at mast and antenna connection plotted versus the percent of available mast modes retained. (Forcing Frequency: 8.95 Hz)

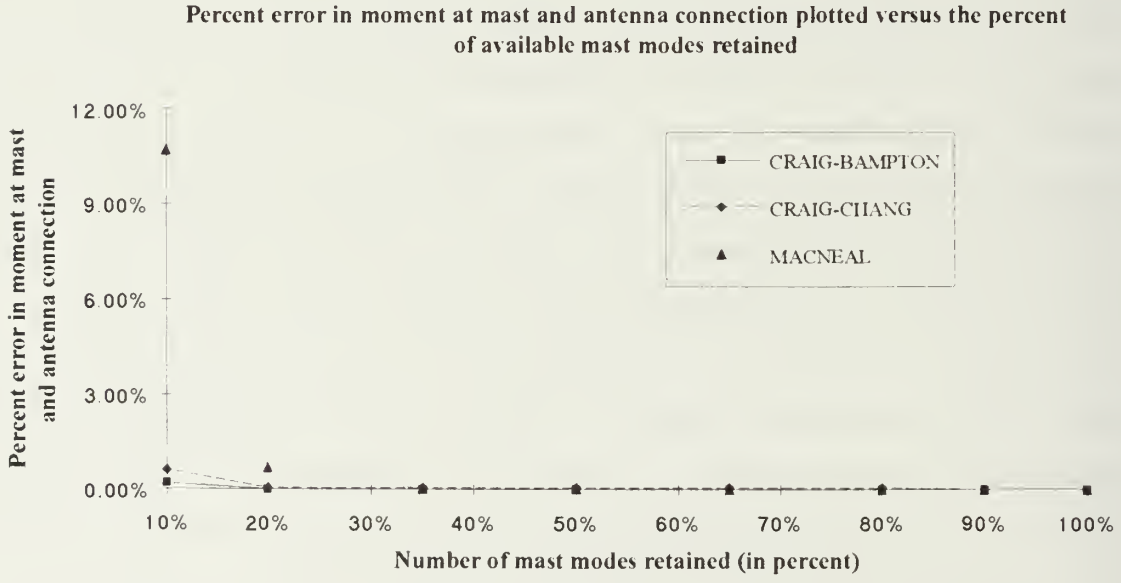

Figure 9: Percent error in moment at mast and antenna connection plotted versus the percent of available mast modes retained. (Forcing Frequency: 8.95 Hz)

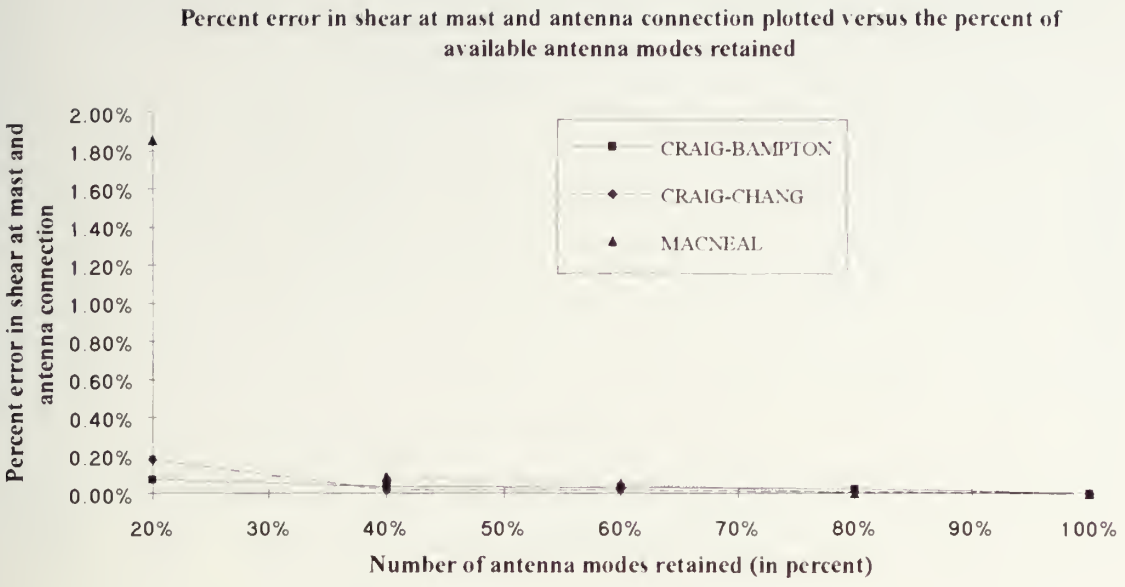

Figure 10: Percent error in shear at mast and antenna connection plotted versus the percent of available antenna modes retained. (Forcing Frequency: 8.95 Hz)

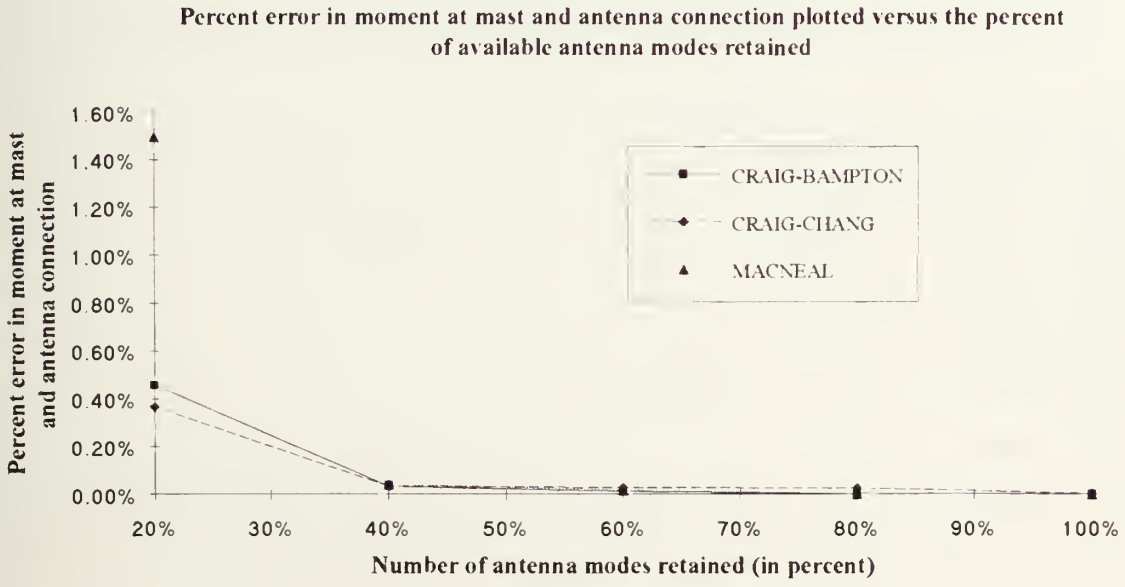

Figure 11: Percent error in moment at mast and antenna connection plotted versus the percent of available antenna modes retained. (Forcing Frequency: 8.95 Hz)

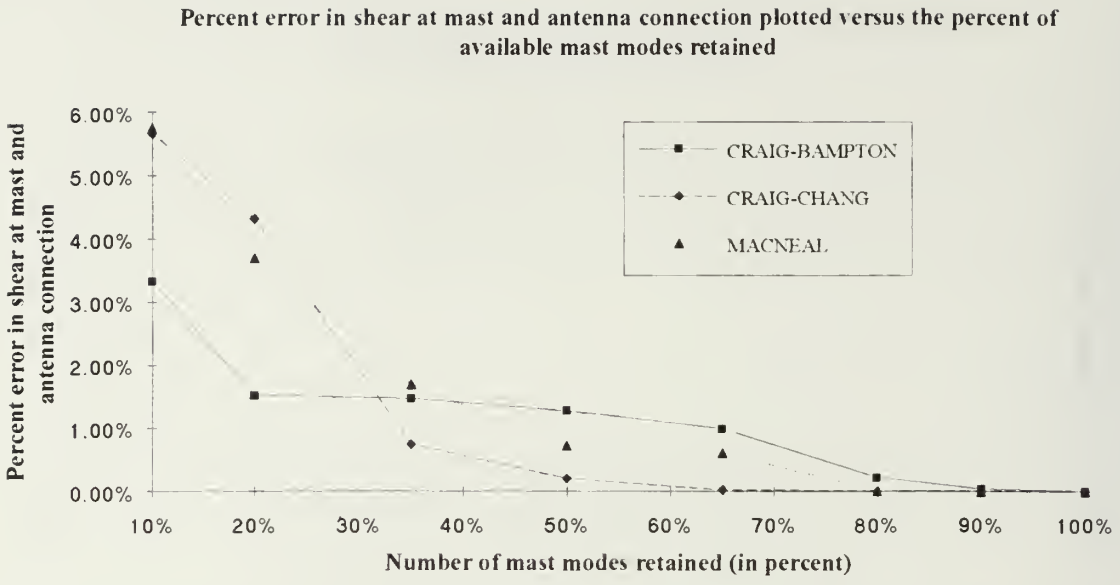

Figure 12: Percent error in shear at mast and antenna connection plotted versus the percent of available mast modes retained. (Forcing Frequency: 219 Hz)

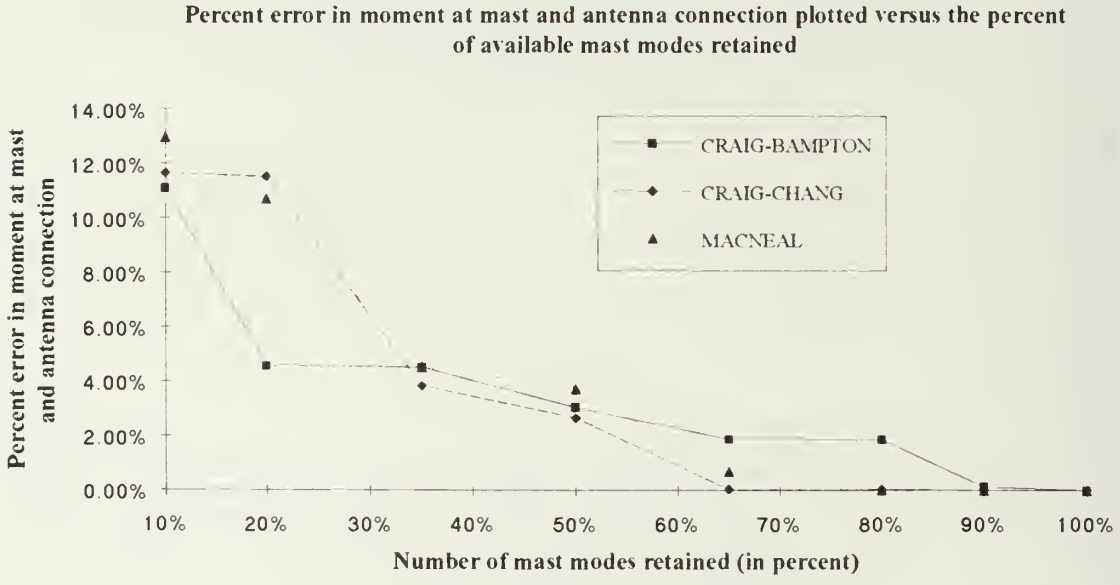

Figure 13: Percent error in moment at mast and antenna connection plotted versus the percent of available mast modes retained. (Forcing Frequency: 219 Hz)

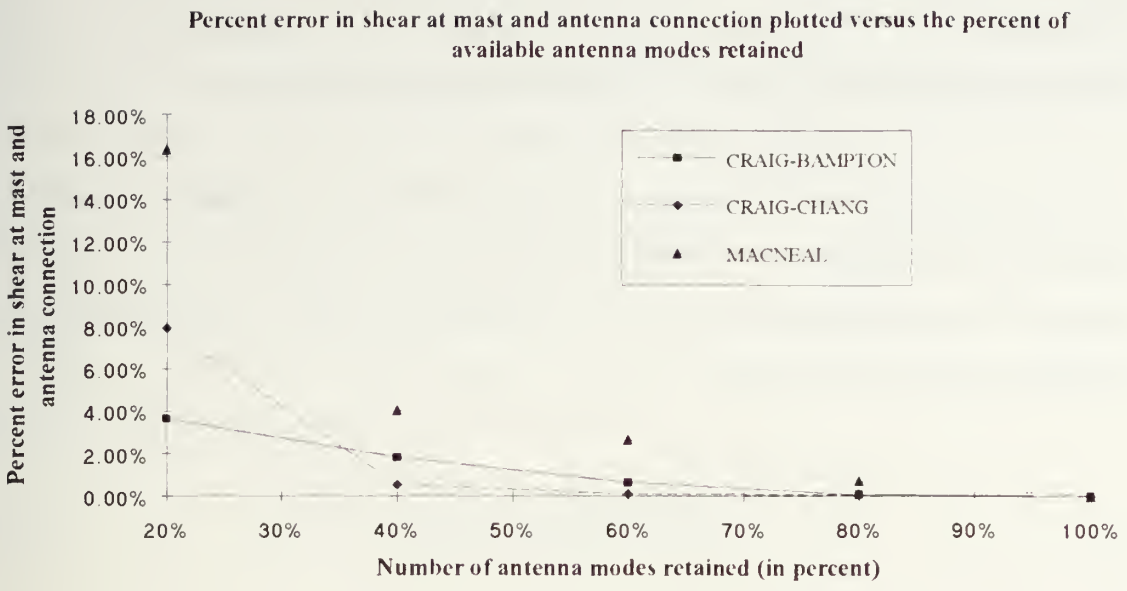

Figure 14: Percent error in shear at mast and antenna connection plotted versus the percent of available antenna modes retained. (Forcing Frequency: 219 Hz)

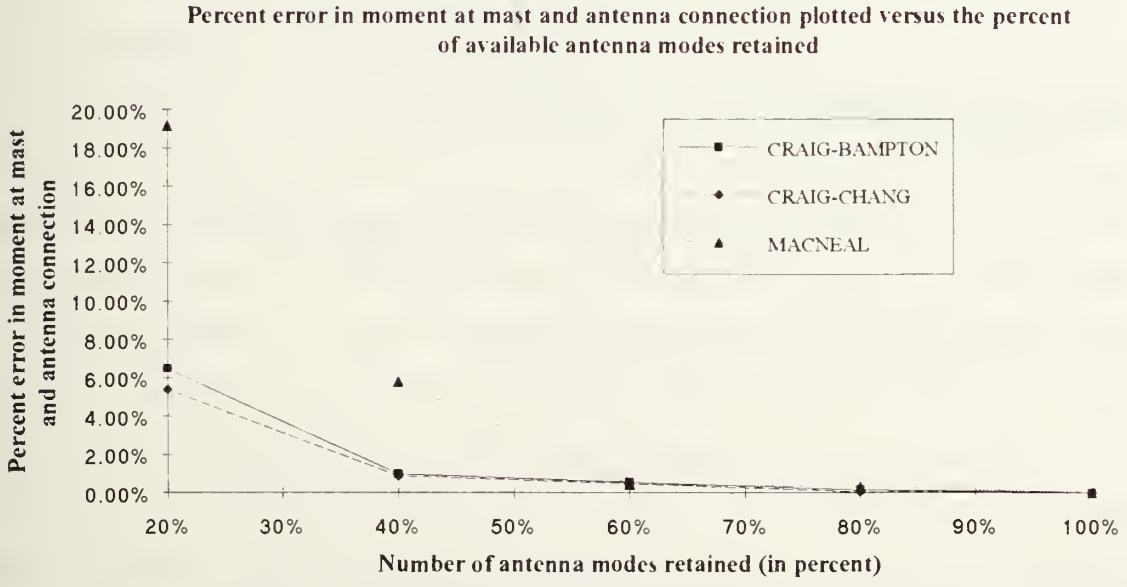

Figure 15: Percent error in moment at mast and antenna connection plotted versus the percent of available antenna modes retained. (Forcing Frequency: 219 Hz)

B. BASE EXCITATION FROM PRESCRIBED DISPLACEMENT

The following derivation is applicable to the base excitation problem, where base displacements (as opposed to base accelerations) are to be prescribed.. As in the base excitation from prescribed acceleration, the derivation starts with the FEM generated mass and stiffness matrices as follows:

$$\begin{bmatrix} M_{OO} & M_{OB} \\ M_{BO} & M_{BB} \end{bmatrix} \begin{Bmatrix} \ddot{x}_O \\ \ddot{x}_B \end{Bmatrix} + \begin{bmatrix} K_{OO} & K_{OB} \\ K_{BO} & K_{BB} \end{bmatrix} \begin{Bmatrix} x_O \\ x_B \end{Bmatrix} = \begin{Bmatrix} F_O \\ 0 \end{Bmatrix} \tag{25}$$

The bottom row is expanded into the following equation:

$$M_{BO}\ddot{x}_O + M_{BB}\ddot{x}_B + K_{BO}x_B + K_{BB}x_B = 0 \tag{28}$$

From Eq. (28), the base acceleration is obtained as follows:

$$\ddot{x}_B = -M_{BB}^{-1}\left[M_{BO}\ddot{x}_O + K_{BO}x_O + K_{BB}x_B\right] \tag{34}$$

From Eq. (25), the top row is expanded to obtain:

$$M_{OO}\ddot{x}_O + M_{OB}\ddot{x}_B + K_{OO}x_O + K_{OB}x_B = F_O \tag{26}$$

Substituting Eq. (34) into Eq. (26) and simplifying, the equation of motion for the internal coordinates as a function of prescribed base displacement is obtained as follows:

$$\left[M_{OO} - M_{OB}M_{BB}^{-1}M_{BO}\right]\ddot{x}_O + \left[K_{OO} - M_{OB}M_{BB}^{-1}K_{BO}\right]x_O = F_O - \left[K_{OB} + M_{OB}M_{BB}^{-1}K_{BB}\right]x_B \tag{35}$$

Notice that the matrix that pre-multiplies the acceleration term has units of mass, and the matrix that pre-multiplies the displacement term has units of stiffness. The matrix that pre-multiplies the base displacement term has units of stiffness. Therefore, all terms of this equation of motion are dimensionally consistent with units of force.

The same modal decomposition procedures described in the base acceleration formulation apply to the base displacement formulation. Since the displacements at the base are prescribed, the base coordinates are no longer degrees of freedom. As in the base acceleration formulation, the time history of the base displacement is taken to be simple harmonic, and is represented by:

$$\{x_B\} = \{X_B\}\sin(\omega t) \tag{36}$$

Numerical convergence examples are provided in the following section. Both examples are similar to the examples presented in the prescribed base acceleration problem.

1. TIP DEFLECTION CALCULATION

The mast and antenna system was subjected to a base excitation where the time history of the displacement of the base coordinates was prescribed. The excitation was performed at a frequency which corresponded approximately to mode 5 (47.26 Hz) of the mast/antenna system. Since the system was modeled without damping, a frequency which corresponded exactly to a natural frequency of the system could not be prescribed. The excitation frequency is equivalent to the mode 5 natural frequency to within 2 decimal places. As in the base acceleration problem, the frequency was arbitrarily selected. The tip deflection of the antenna was calculated and percent error in tip deflection was plotted versus percent of available component modes retained (see figures 16 and 17). The calculations were performed twice. Mast modes were truncated in the first calculation, and antenna modes were truncated in the second calculation. All three procedures yielded accurate results in both the mast and antenna truncation tests. When the mast/antenna

system was excited at mode 5, the Craig-Chang and MacNeal procedures provided very similar results for both the mast truncation and antenna truncation. As was determined in the tip deflection calculations of the base acceleration problem, the Craig-Bampton procedure yielded the best results using fewer modes than did the Craig-Chang and MacNeal procedures in both truncation tests. This again could possibly be due to the combination of fixed interface normal modes and static constraint modes providing a better representation of prescribed base displacement than the combination of free interface normal modes and residual flexibility modes. However, all three provided accurate results and at a cheaper cost than the FE model.

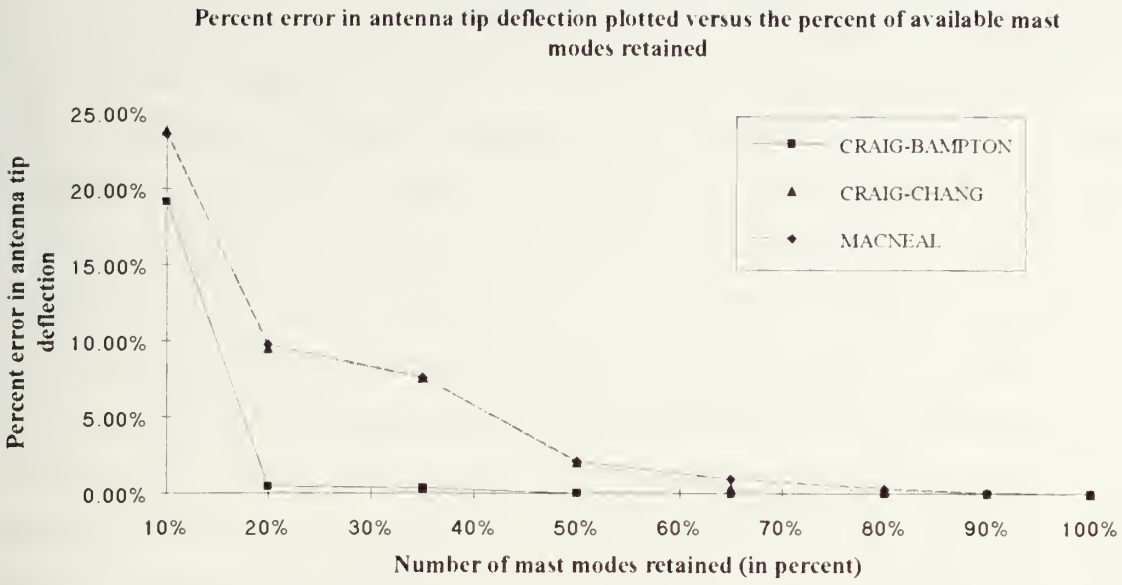

Figure 16: Percent error in antenna tip deflection plotted versus the percent of available mast modes retained (Forcing Frequency: 47.26 Hz)

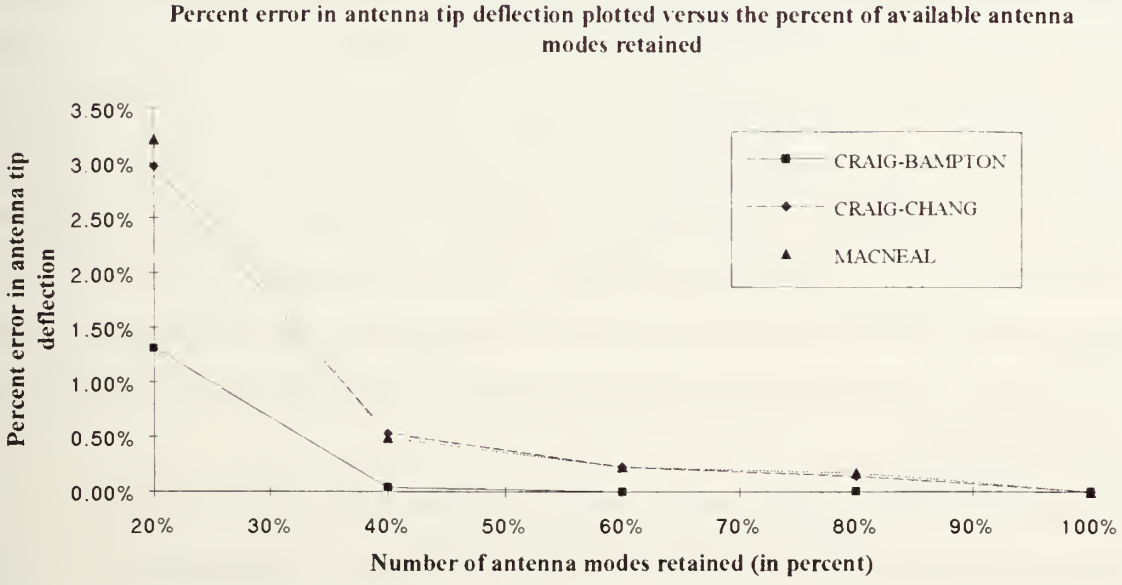

Figure 17: Percent error in antenna tip deflection plotted versus the percent of available antenna modes retained. (Forcing Frequency: 47.26 Hz)

2. MOMENT AND SHEAR CALCULATION

Percent error in shear and moment at the mast and antenna connection were plotted versus the percent of available component modes retained (see figures 18-21). The base excitation was conducted again at 47.26 Hz Similar results were obtained in the shear and moment calculations as were obtained in the tip deflection calculations. The Craig-Bampton procedure provided more accurate results using fewer modes than the Craig-Chang and MacNeal methods. The convergence rate of the Craig-Chang and MacNeal methods were almost identical in the mast mode truncation. When the mast was excited at mode 5, all three yielded excellent results in the antenna mode truncation analysis. However, the Craig-Bampton procedure converged more quickly than the other methods. It appears that the combination of fixed interface normal modes and static constraint modes lead to a higher rate of convergence in determining tip deflection and antenna/mast shear and moment calculations Although all three procedures initially had a higher percentage error when truncating mast modes, than when truncating antennae modes, they all provide as accurate if not more accurate results than the antenna truncation at less cost in terms of computations. It is also noteworthy to compare the computational cost in retaining mast modes versus retaining antenna modes in predicting accurate system response. For example, in the shear calculation when the mast was excited at mode 5, the Craig-Chang procedure yielded a percentage error of 2.1% while using $1.66 \cdot 10^6$ FLOPS during the mast mode truncation test. During the antenna mode truncation test, the Craig-Chang procedure yielded a percentage error of 2.03% using $1.89 \cdot 10^6$ FLOPS.

Since the impact of shock waves on the mast/antenna system are typically of low frequency, and as can be seen from the results of the prescribed base acceleration and base displacement examples provided, it is recommended that the Craig-Bampton component mode representation be used to synthesize the mast and antenna system.

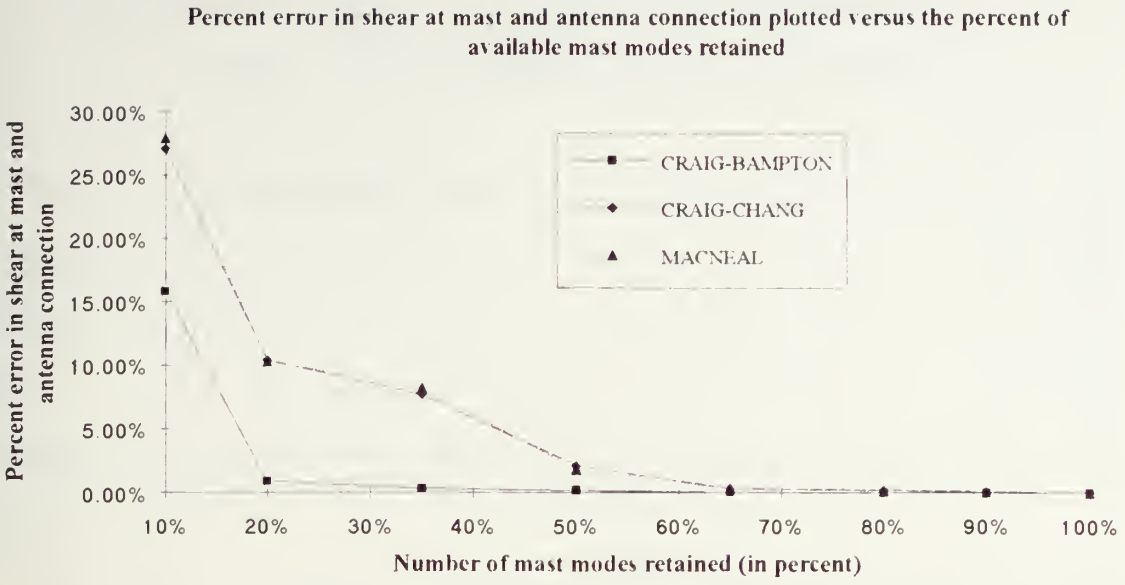

Figure 18: Percent error in shear at mast and antenna connection plotted versus the percent of available mast modes retained. (Forcing Frequency: 47.26 Hz)

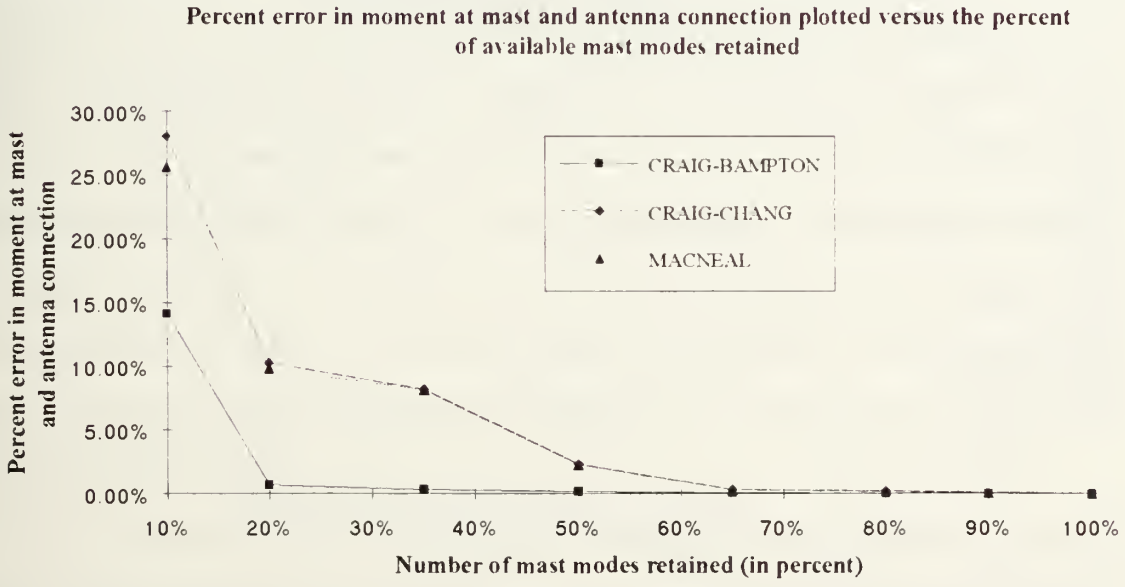

Figure 19: Percent error in moment at mast and antenna connection versus the percent of available mast modes retained. (Forcing Frequency: 47.26 Hz)

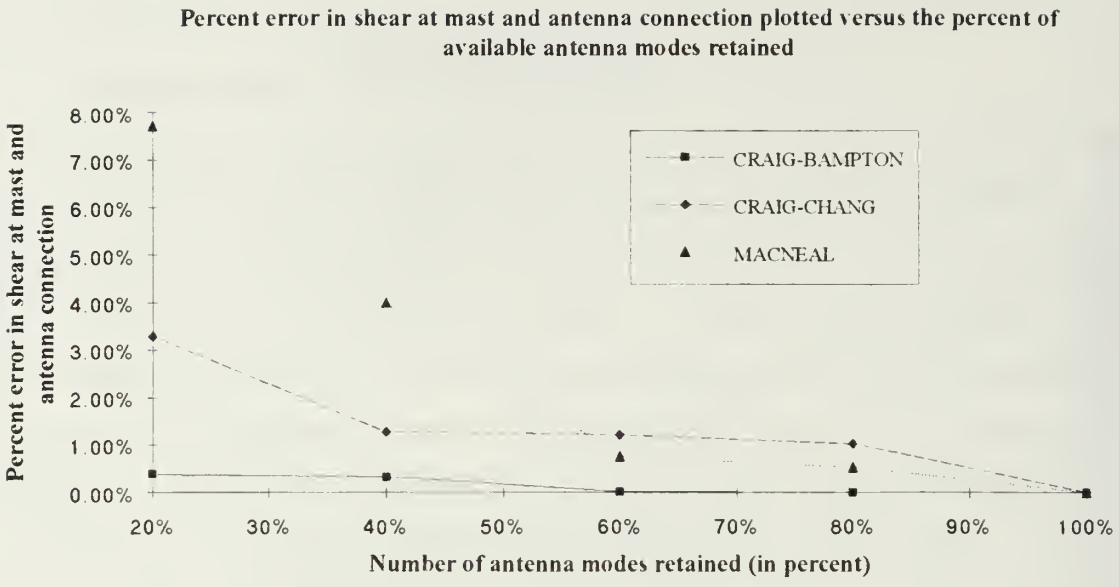

Figure 20: Percent error in shear at mast and antenna connection plotted versus the percent of available antenna modes retained. (Forcing Frequency: 47.26 Hz)

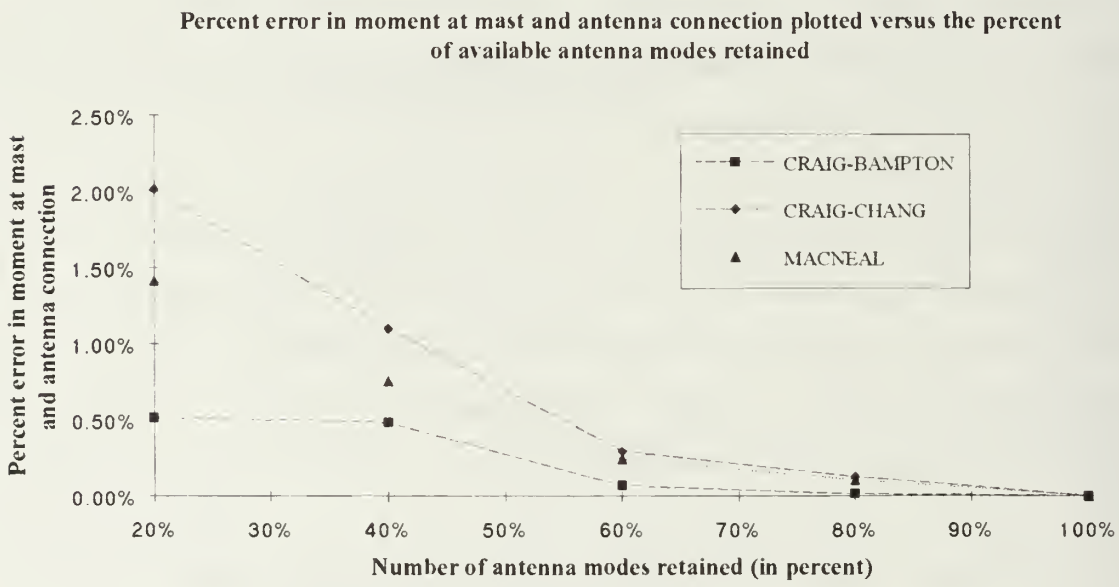

Figure 21: Percent error in moment at mast and antenna connection plotted versus the percent of available antenna modes retained. (Forcing Frequency: 47.26 Hz)

VI. PRELIMINARY RESULTS AND CONCLUSIONS

The survivability of shipboard combat systems equipment is paramount to the warfare fighting capability of the ship and her crew. Should a fire control radar, or any vital topside combat systems equipment fail as a result of an induced shock wave, the ship's war fighting capacity would be crippled. However, using proven structural dynamics techniques, the design engineer can design the mast/antenna system in such a manner as to minimize risk of failure.

As seen in this report, the mast and antenna can be treated as separate substructures, and using CMS, can be assembled as a mast/antenna system, from which dynamic response to base excitation can be calculated. Treating each antenna as a substructure, allows the cataloging of the various antennae. A selected antenna can be "plugged" into various locations along the mast until a suitable dynamic response is obtained. As has been demonstrated herein, CMS in conjunction with FE modeling provides rapid and accurate results at a computational cost significantly less than standard FE modeling. The mock mast/antenna system used in this report consisted of only 17 elements and a total of 51 degrees of freedom. Although the results that were obtained on this "small" model were accurate and required small compute times, the same benefits demonstrated herein can be expected with larger models, specifically those that will be used to represent real mast and antennae systems.

All three methods yield results that are accurate and more computationally efficient than standard FE modeling. However, from the results obtained, it is recommended that the Craig-Bampton component mode representation be used to synthesize the mast and antennae system. As mentioned previously, the mast is excited typically by low

frequencies. Since the Craig-Bampton procedure yielded more accurate results while using fewer component modes than the other methods, the Craig-Bampton procedure is the substructure coupling formulation of choice due to good accuracy and ease of implementation. Additionally, the NASTRAN superelement scheme contains the Craig-Bampton component mode representation as a solution path to dynamic analyses.

REFERENCES

1. Corbell, R.D., *Shock Qualification of Combat Systems Equipment Using Tuned Mounting Fixtures on the U.S. Navy Mediumweight Shock Machine*, Master's Thesis, Naval Postgraduate School, Monterey, California, June 1992.

2. NKF Report 8969-AEA/1, *Modal Test and Shock Response Analysis of the LHD-1 Foremast and the SPA-72 Antenna and Platform*, by NKF Engineering, April, 1993.

3. Colub, G.H., and Van Loan, C.F., *Matrix Computations*, pp. 231, Johns Hopkins, 1983.

4. Craig, R.R., *Structural Dynamics, An Introduction to Computer Methods*, pp. 447, John Wiley and Sons, 1981.

5. Craig, R.R., *Structural Dynamics, An Introduction to Computer Methods*, pp. 491, John Wiley and Sons, 1981.

6. Chang, C.J., *A General Procedure for Substructure Coupling in Dynamic Analysis*, Ph.D. Dissertation, University of Texas at Austin, Austin Texas, 1977.

INITIAL DISTRIBUTION LIST

		No. of Copies
1.	Defense Technical Information Center Cameron Station Alexandria, Virginia 22304-6145	2
2.	Library, Code 52 Naval Postgraduate School Monterey, California 93943-5002	2
3.	Professor J. H. Gordis, Code ME/Go Department of Mechanical Engineering Naval Postgraduate School Monterey, California 93943	3
4.	Professor Y. S. Shin, Code ME/Sg Department of Mechanical Engineering Naval Postgraduate School Monterey, California 93943	1
5.	Naval Engineering Curricular Office, Code 34 Naval Postgraduate School Monterey, California 93943-5000	1
6.	Mr. Mark McClean Code 03K21 Naval Sea Systems Command 2531 Jefferson Davis Highway Arlington, VA 22242-5160	2
7.	Mr. Joel Bloom Staff Scientist Office of the Secretary of Defense OSD/ODDRE/Live Fire Test Room 3E1060, The Pentagon Washington, D.C. 20301	2
8.	Mr. Vic DiRienzo Code 03K21 Naval Sea Systems Command 2531 Jefferson Davis Highway Arlington, VA 22242-5160	1

9.	Mr. Fredrick Costanzo Naval Surface Warfare Center Underwater Explosion Research Division Norfolk Naval Shipyard, Bldg. 369 Portsmouth, VA 23709	1
10.	Mr. Michael Riley Naval Surface Warfare Center Underwater Explosion Research Division Norfolk Naval Shipyard, Bldg. 369 Portsmouth, VA 23709	1
11.	Mr. John Schell Naval Sea Systems Command Department of Navy Washington,D.C. 20362-5101	1
12.	Mr. Jerry Hill NKF Engineering, Inc. 4200 Wilson Blvd., Suite 900 Arlington, VA 22203-1800	1
13.	Dr. E. Thomas Moyer, Jr. NKF Engineering, Inc. 4200 Wilson Blvd., Suite 900 Arlington, VA 22203-1800	1
14.	LT Lynn J. Petersen U. S. Navy 387B Bergin St. Monterey, CA 93940	1